INTERNATIONAL JOURNAL OF AUTOMOTIVE AND MECHANICAL ENGINEERING
ISSN: 2229-8649 e-ISSN: 2180-1606
VOLUME 23, ISSUE 2, 2026, 13716 - 13737
DOI: https://doi.org/10.15282/ijame.23.2.2026.17.1036

REVIEW ARTICLE

Process optimisation in laser metal deposition of high entropy alloys

Agbaye Ignatius Uyabemem[1], Aini Zuhra Abdul Kadir[2], Tuty Asma Abu Bakar[2,3]*

[1]Department of Metalworks Technology Education, Federal College of Education (Technical), Asaba, Delta State, Nigeria
[2]Department of Materials, Manufacturing & Industrial Engineering, Universiti Teknologi Malaysia, 81310 Johor Bahru, Johor, Malaysia
[3]Centre for Advanced Composite Materials (CACM), Universiti Teknologi Malaysia, 81310 Johor Bahru, Johor, Malaysia

Abstract – Laser metal deposition (LMD) has become a compelling technique for fabricating high-entropy alloys (HEAs). However, its adoption on a commercial scale is limited, hindered by process-related defects and difficulty in controlling numerous interacting parameters. This review examines defect formation, process parameter-property relationships, and optimisation approaches for LMD-fabricated HEAs. The findings establish that the quality of LMD part is governed by about 39 process variables, including 13 key process parameters, out of which laser power, scan speed, powder feed rate, beam diameter, layer thickness, overlap fraction, and shield gas flow rate exercise dominant effects on the melt-pool stability, microstructure and mechanical properties. Cracking, lack of fusion, gas porosity, surface-connected porosity, and gas porosity constitute the main defects, with lack of fusion reported when scan speed deviates from the optimum range by more than 15%. Evidence from reviewed studies indicates that increasing laser power from 600 to 800 W enhances hardness from 200 to 600 HV in AlCoCrFeCu HEA, and from 500 to 850 HV in AlTiCrCoNi HEA. Optimised process windows for fabricating defect-free CoCrFeMnNi are 400-600 W and 10-30 mm/s. Nevertheless, excessive layer thickness of about 300 μm results in reduced elongation from 11.45% to 2.0%. Advanced optimisation techniques enhanced the reliability of prediction: Taguchi-grey relational analysis obtained 0.95% deviation, response surface methodology produced 5.27%-10%, and machine learning approaches achieved R^2 values between 0.97-1.00, including phase-prediction precision of 98.5%. In general, hybrid machine learning, physics-based optimisation, and digital twin frameworks present the most compelling way for attaining defect-free, high-performance LMD-produced HEAs.

Article History
Received : 22 September 2025
Revised : 20 January 2026
Accepted : 29 April 2026
Published : 30 June 2026

Keywords
Process parameters
Laser metal deposition
High entropy alloy
Optimisation
Additive manufacturing

1. Introduction

High entropy alloys (HEAs), also called multi-principal element alloys, are a group of alloys made up of five or more principal elements, with constituent elements of 5 to 35 wt.% composition, or equal atomic ratios. They have attracted growing interest and development activities from both academics and industrial players [1]-[2]. They exhibit four core effects that give them an edge over conventional alloys in formability and damage tolerance [3]. It has been reported that the core effects- lattice distortion, high entropy [4], [5], sluggish diffusion [6], and cocktail effect- are the factors contributing to the superior thermal, physical, and mechanical properties [7]. Therefore, HEAs exhibit high strength and good ductility [8], superior hardness and wear resistance [9], excellent corrosion and oxidation resistance [10], [11], as well as high- and cryogenic-temperature stability [12]. Vacuum and induction arc melting are the predominant methods for fabricating HEAs. However, they are only used in academic and industrial research laboratory studies due to poor strength and hardness in the as-cast state, in addition to the high cost of equipment for commercial production [13]. The laser metal deposition additive manufacturing technique is characterised by rapid cooling and low temperature gradient solidification, and flexibility for fabricating complex shapes and is adapted for manufacturing HEA parts of heterogeneous structures with superior strength, wear and corrosion properties. LMD technology has become a promising medium for fabricating premium alloys owing to its low dilution rate, rapid cooling and solidification rates, and the ability to directly repair damaged surfaces of parts [13]. In the LMD process, the main raw material, or feedstock, is metal powder, which is supplied by a carrier gas through coaxial ducts, then melted by a high-temperature laser and printed on a substrate layer by layer.

Beyond the unique advantages of LMD, the ability to safely produce high-quality parts depends largely on controlling the process parameters and maintaining proper environmental conditions. In the LMD process, the thermal cycle controls the microstructure and mechanical properties of the deposited part and is highly influenced by the process parameters (powder feed rate, laser power, and laser scanning pattern/strategy [14]). Understanding the interactions among LMD process parameters, process conditions, and mechanisms is crucial, as they work in combination to produce parts of desired quality (defect-free and damage-tolerant). These factors or parameters are often myriad and controlling them is more complex and herculean. For better understanding, these factors have been grouped into five categories: powder/material related, machine specifications, process and environmental state, process parameters, motion and process control, as illustrated in Figure 1.

***CORRESPONDING AUTHOR** | Tuty Asma | ✉ tuty@utm.my

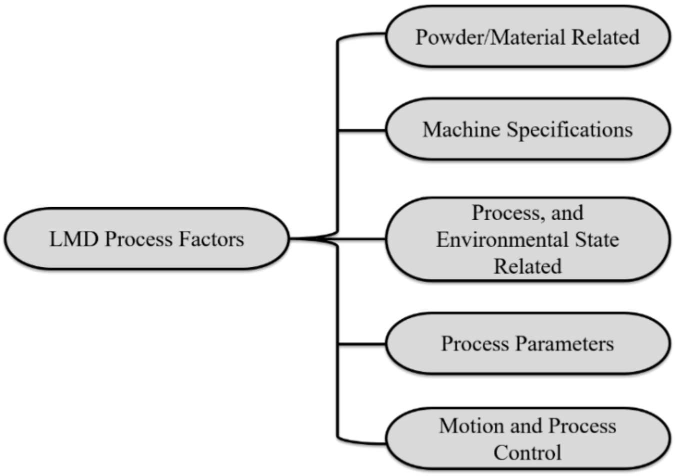

Figure 1. Categorisation of LMD process factors

Among the various process factors and variables, process parameters are the most critical in determining the quality of the fabricated part [15], [16]. The laser metal deposition process is complex, as fabricating safe, defect-free and high-quality deposits depends on the interplay of about 39 variables, with process parameters constituting about 13 of them [17]. According to some studies, among other parameters, laser power, power feed rate, laser scan speed/velocity, and scanning pattern/strategy have a greater impact on the value of the deposited component [18]. Several studies have established that proper selection and optimisation of process parameters are essential to obtaining desired material properties in LMD depositions [14], [19]. The most traditional methods used in these studies to optimise these input parameters include the design of experiments (DoE) technique, employing statistical techniques such as regression analysis, Taguchi orthogonal experimental methods, response surface approach, as well as numerical simulation, enabling them to predict and adopt the optimum process parameters [20], [21]. In the last decade, researchers have further explored the possibility of predicting the optimal process parameters, microstructure, and properties of LMDed HEAs using artificial intelligence-aided machine learning algorithms [22]. These methods offer unique advantages over traditional statistical methods, owing to their multi-objective inclusivity and superior convergence compared with other statistical optimisation methods. Some of these methods include Artificial Neural Networks [23], [24], particle swarm optimisation [25], Non-dominated Sorting Genetic Algorithm II [19], and Support Vector Regression [26].

This study reviews progress in optimising LMD parameters to limit defects and enhance the quality of fabricated HEAs. It starts by reviewing the defects associated with the LMD process. It summarises the key variables that contribute to defects in the LMD process and the remedies to mitigate them, as identified in the reviewed studies. The study further summarises the methods researchers use to optimise process parameters, ranging from conventional to multi-objective intelligent methods, and reviews their advantages and limitations. Based on the level of success observed in the reviewed studies, this study provides an outlook on progress in optimisation procedures for LMD processing of HEAs. This review is expected to serve as reference material for prospective research on the additive manufacturing of high-quality HEAs via LMD.

2. Defects in the LMD Process

The laser deposition process largely depends on the complex interplay of numerous process conditions and variables that, if not properly controlled, can affect the quality of the deposited or fabricated part. Defects are physical imperfections in fabricated parts that require correction [17], [27]. HEAs, due to their complex microstructure and multi-principal element composition, are prone to defects during laser metal deposition. These defects can be categorised into five groups:

2.1 Crack Defects in the LMD Process

Cracks in laser metal deposition occur in the deposited parts mostly due to high temperature gradients. Cracking of the components occurs due to the inability to accommodate solidification shrinkage and thermal contraction under a high solidification temperature gradient [27], [28]. Cracks also develop due to uncontrolled thermal stresses and strains, as well as uncontrolled microstructural and phase evolution, which normally cause shrinkage in the interdendritic grain zones [29]. In LMD, crack formation is influenced by critical parameters such as laser power and scan speed; higher laser energy can generate thermal stress, leading to crack initiation. An excessive laser scan speed can result in a lack of fusion, leading to crack formation [30]. Layer thickness and overlap are also critical to crack formation, as large thicknesses can lead to heat accumulation and higher cooling rates, which can create interlayer cracking [31]. Cracks can also develop due to the elemental composition of the fabricated alloys, particularly when the amounts of Carbon (C) and Sulphur (S) are high, which can lead to grain boundary segregation [32]. Cracks in the LMD of HEAs can also result from the high oxygen content of the feed powder and high laser heat input during deposition [33]. The strategies for crack reduction include optimal control of process parameters, build-surface preheating, and controlled cooling rates [33]. The main causes of cracks in the LMD process and possible remedies as studied by various researchers are summarised in Table 1.

Table 1. Common LMD defects and remedies

Defect	Causes	Remedies	References
Cracks	Thermal stresses due to a high temperature gradient while cooling	Adopting an optimum cooling rate	[34]
	Inadequate material properties	Preheating the substrate or base metal	[34], [35]
	High laser heat input	Reducing laser heat input	[36]
Cracks	High oxygen content of HEA powder	Reduce oxygen content by drying the powder and performing LMD in an argon environment	[36]
	Coarse columnar grain precipitated.	Adopting optimum inter-layer pause (IP) time	[31]
Lack of fusion	Inappropriate laser power	Adjusting laser power optimally	[34], [37]
	Poor powder quality	Proper powder handling and preparation	[38]
	Poor wettability from oxide film formation and balling effect	Drying the powder and optimising scan speed	[39]
Gas porosity	Gas entrapped during solidification	Reducing the gas content in the chamber	[34]
	High moisture content of powder	Adequate drying of powder, introducing oxygen-trapping additives	[40]
Impurities	Contaminants during processing	Clean material handling, Laser re-melting	[41]
	Poor powder quality	Use of high-quality powder	[35]
Surface-connected porosity	Rapid cooling rate	Using controlled cooling methods	[34]

2.2 Lack of Fusion

A lack-of-fusion (LoF) defect is a common anomaly in laser metal deposition, characterised by discontinuities in the deposited material due to inadequate bonding to the substrate or preceding layers [27]. Lack-of-fusion occurs in laser metal deposition, where powder particles fail to fully fuse due to low laser power, large layer thickness, high cooling rate, and inappropriate processing conditions [34]. Majunder et al. [38] reported that varying the scan speed >15% from the optimal value triggers the LoF defect. In LMD of HEAs, LoF can also arise from the different melting temperatures of the HEA powder's compositional elements [42]. Energy area density, if not optimally selected, can also cause a lack-of-fusion defect [37]. There are also material-related factors responsible for the lack-of-fusion defect, such as poor powder wettability, oxide formation, contamination, and an improper powder particle-size distribution [37], [39], [43]. Lack-of-fusion can be identified using process-monitoring methods such as X-ray computed tomography [44], ultrasonic non-destructive testing [45], metallographic examination [34], and mechanical testing [46]. Optimising process parameters can significantly mitigate the LoF defect [47]. A modern human-learning approach for real-time prediction of fusion failure achieves up to 90% accuracy [48]. Some common causes of LoF and their remedies identified in the reviewed studies are summarised in Table 1.

2.3 Gas Porosity

Gas porosity is another common problem associated with laser metal deposition. The nature and causes of porosity in the metal additive manufacturing processes, including LMD, are the same. It is a major concern because it significantly affects the mechanical properties and structural performance of the alloys produced. Understanding the mechanisms and factors that trigger porosity is important for fabricating components with the desired quality and reliability. Porosity can come from the original powder [17], gas entrapment [49], lack-of-fusion and keyhole pores [50]. According to Dobbelstein et al.[50], pores can develop in LMD during the fabrication of high-melting-point alloys with wide solidification ranges, where the evaporation of lower-melting-point elements induces shrinkage and interdendritic porosity. Appropriate control of process parameters limits porosity. A high laser energy enhances effective melting and limits pore formation. Adopting a high powder flow rate and uniform layer thickness can also help prevent voids [51]. In their findings, Gao et al.[40] established that introducing material additives such as titanium boride (TiB_2) particles reduces porosity and crack effects through Orowan strengthening.

2.4 Impurities

The laser metal deposition process is prone to numerous impurities, which can degrade both the physical and mechanical performance of the resulting material [34]. Defects can arise as inclusions of oxygen and nitrogen trapped within the metal matrix during deposition [42]. Uneven segregation of alloying elements during deposition can also introduce impurities that distort the alloy's mechanical properties and structural integrity [52]. Voids from entrapped gas can act as impurities, weakening the deposited material [53]. Surface-active impurities cause oscillatory flows in the melt pool, which interfere with solidification and create non-uniform surface morphology [54]. The presence of impurities reduces ductility and toughness. It causes cracks and incomplete fusion, which affect both the strength and the surface quality of the component produced [53]. The problem of impurities can be overcome through advancements in process control and material selection to improve outcomes in laser metal deposition [55].

2.5 Surface-Connected Porosity

Surface-connected porosity is another detrimental defect in LMD that affects the physical properties of the produced part, such as permeability and absorption [56]. These bubbles are created by trapped gases during solidification, resulting from poor design parameters [57]. Reducing surface porosity is essential for enhancing the component's quality and mechanical properties through post-processing [58], nanoparticle injection [59], powder deoxidation [60], and temperature control [61]. A summary of the defects, their cause, and remedies is presented in Table 1.

3. Influence of LMD Processing Parameters

Selecting the right process parameters is critical to the quality of printed parts in laser additive manufacturing, particularly in LMD. They influence the evolution of microstructure, consequently affecting mechanical properties and the overall quality of the metallic alloy [62]. The most dominant process parameters are laser power, scan speed, and powder feed rate; they govern the thermal cycle, which determines the quality characteristics of the printed part [63], [64]. Apart from these three parameters, this review paper will also discuss the influence of laser beam diameter, laser thickness, overlap fraction and shield gas flow rate.

3.1 Laser Power

The laser power intensity determines the properties of the deposited part, including porosity, hardness, bonding strength, and wear resistance. Reports indicate that, especially for high-melting-point metals, higher laser power facilitates adequate melting of the feedstock material (powder or wire), effective adhesion, a dense microstructure, and greater hardness of the deposited alloy [65]. For lower-melting metallic alloys such as copper and aluminium, higher laser power may initially refine grains; however, excessive power can cause overheating and grain coarsening, reducing the metal's electrical and corrosion resistance [66]. Wang et al. [67]reported improved mechanical properties, including higher hardness and wear resistance, by increasing laser power to a peak of 1400 W in an LMDed Fe-Ni-Ti alloy. Similarly, Liu et al. [68]reported lower wear rates for $Cu_{45}ZrAl_6Ti_4$ deposited at the optimal laser power. The study reported that higher laser power has yielded tensile strength comparable to that of low-power processing, indicating that, despite grain coarsening, higher power can improve the mechanical properties of the deposited alloy. It has been observed that higher laser powers favour better mechanical properties and reduce defects. Still, they can also increase grain coarseness, which affects both the alloy's electrical conductivity and corrosion resistance. Therefore, optimising the laser power parameter is important for achieving high-quality deposition.

3.2 Laser Scan Speed

The laser scan velocity is a key parameter that significantly influences the microstructural evolution and overall structural performance of the alloy fabricated via LMD. Changes in laser scan speed can affect defect formation, grain size, and phase distribution, thereby influencing the mechanical properties of the deposited part [69]. In microstructural evolution, a higher scan speed yields finer microstructures and higher hardness and wear resistance [70]. Using higher laser scan speeds, especially for high-melting metals, can enhance hardness. However, excessive scan speed can lead to retained austenite in Fe-based alloys, thereby decreasing wear and corrosion resistance, as well as the material's hardness [71].

3.3 Powder/Wire Feed Rate

The rate at which the feedstock material (wire or powder) is fed significantly affects the quality and performance characteristics of laser metal-deposited components, such as laser density and scan speed. The emphasis in this study is on the powder-blown LMD system. Liu et al. [68] increased the powder feed rate to 90 g/min and obtained a crack-free deposit. Powder feed rate has been shown to influence grain size, reducing it and enhancing a finer microstructure, thereby improving mechanical properties [72]. However, Kim and Shim [73] reported that a low powder feed rate of 3.5 g/min led to defect-free deposition, underscoring the importance of understanding material characteristics before selecting the powder feed rate. The build rate in LMD is also highly dependent on the powder feed rate, necessitating an optimal feed rate for efficient manufacturing [74].

3.4 Diameter of Laser Beam

The diameter of the laser beam, or the nozzle diameter in LMD, should not be overlooked, as it influences the microstructural characteristics of the produced material. Studies indicated that smaller beam diameters, such as 0.75mm, result in rapid cooling, which triggers fine-grain growth and higher dislocation densities, thereby improving mechanical properties [75]. According to Vidergar et al. [76], larger laser diameters ensure a stable molten pool and reduce powder splashing, thereby reducing powder waste and improving the surface finish of the printed material. For LMD, process stability and efficiency: a larger beam diameter yields higher efficiency at lower laser density.[76]. However, the diameter of the laser beam largely depends on the specific application. For example, repairing complex geometries, such as turbine blades, will require an optimal diameter that matches the blade thickness [75], [77]. While larger beam diameters improve productivity and material efficiency, they may compromise microstructural homogeneity and component strength. Thus, the choice of beam diameter often depends on the specific requirements or intended application. An example of a complex-shaped part for LMD repair requiring a specific nozzle diameter is shown in Figure 2.

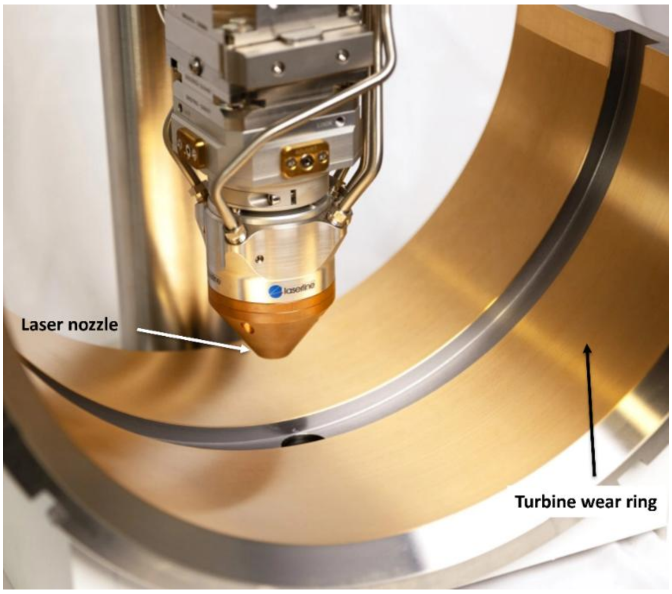

Figure 2. Damaged parts under LMD repair

3.5 Layer Thickness

The thickness of deposited layers in laser metal deposition plays a crucial role in mitigating defects, microstructural changes, and in determining the mechanical properties of the produced alloy. A thicker layer may increase build rates, but if not well controlled, it can lead to defects [78]. Li et al. [79] also confirmed that thicker-layer deposition increased productivity and resulted in larger melt pool dimensions but introduced defects. Studies also indicated that thicker layer depositions adversely affect the microstructure and can enhance pore formation [80]. Brudler et al. [78] reported that increasing the thickness of the deposited layer from about 60 to 300 µm affected the mechanical properties of Ti6Al4V, as the elongation dropped from 11.45 to 2.0%, which was attributed to lack-of-fusion porosity.

3.6 Overlap Fraction

The overlap fraction significantly affects the quality and performance of laser-metal-deposited parts and must be carefully selected. It indicates how successive layers overlap during the LMD process. Bu et al. [81] found that increasing the overlap rate to about 80% refined the grain size to about 1.14 µm, resulting in a homogeneous microstructure. A well-controlled, uniform overlap will facilitate the formation of stable phases [82]. Overlap fractions, when well maintained, can improve mechanical properties, including hardness, wear resistance, and corrosion resistance, due to good adhesion and low porosity [82], [83]. However, care must be taken when selecting this parameter, as excessive overlap fraction can lead to porosity and an irregular microstructure, which will be detrimental to the integrity and performance of the deposited part.

3.7 Shield Gas Field Rate

The shield gas field prevents oxidation and influences the cooling rate during deposition, thereby homogenising the microstructure through stable solid solutions, which improves the strength of the deposited components [84]. Shield gas controls oxidation, limiting defects and enhancing the mechanical and corrosion properties of the fabricated product [85]. An appropriate gas-shield rate will also ensure a uniform deposition layer and improved bonding and adhesion, thereby enhancing the wear and corrosion behaviour of the deposited parts [86]. It is important to understand the balance of this parameter because an excessive gas field rate can generate turbulence and an inconsistent deposition process, both of which are detrimental to the quality of the LMD-produced alloy.

3.8 Fabrication Processes, Alloy Compositions and Optimum Process Parameters

The optimal values of process parameters vary across HEA fabrication processes, as each operates under distinct thermomechanical conditions and exhibits different sensitivities to parameters. For instance, in Laser Powder Bed Fusion (LPBF), energy density and laser scan speed are the most sensitive parameters. Since the powder is pre-applied to the bed at a predetermined thickness, only the laser power and scan velocity can be varied. High laser power is needed for deeper penetration and adequate melting. Nonetheless, excessive power causes keyholing, whereas a lack-of-fusion and the development of pores occur at low laser power [87]. Laser Metal Deposition (LMD), which involves feeding powder or wire, requires a larger melt pool, higher power, and a moderate cooling rate, and will require different optimal values than those for LPBF [88]. The synergistic control of laser power and scan speed will enhance the stability of melt pool dynamics and thermal gradients.

Apart from the processing technique, the composition of the HEA also determines the optimal fabrication parameters. Optimum values of process parameters can vary across different HEA compositions. Because HEAs consist of multiple principal elements with distinct thermal, mechanical, and phase characteristics, optimising synthesis parameters depends largely on the alloy composition. For example, Dada et al.[89] investigated the effect of processing parameters on two compositional HEAs (Al-Co-Cr-Fe-Ni-Cu and Al-Ti-Cr-Fe-Cu-Ni), fabricated through LMD. The authors found that increasing laser power from 600 to 800 W increased the hardness of the AlCOCrFeNiCu alloy by 300% (200 to 600 HV). In contrast, the other alloy (AlTiCrFeCoNi) showed only a 70% increase in hardness (500 to 850 HV). Though the increase rate is low for AlToCrFeCoNi, the value of hardness was higher than that of AlCoCrFeNiCu due to the presence of Ti, which improves strength by encouraging the growth of laves phases. Therefore, the optimal values of the process parameters vary with alloy composition.

3.9 Melt Pool Dynamics, Dendrite Arm Spacing, Mechanical Anisotropy and Parameter Optimisation

In LMD technology, the melt-pool characteristics, such as shape, molten-metal flow, and temperature distribution, are crucial to how the deposited layer melts and solidifies [88]. The magnitude and control of critical variables such as laser power, scan speed, and powder feed rate influence the size and stability of the melt pool, as well as temperature gradients and solidification rates during the deposition process [88]. Scan strategy/pattern, spot size diameter, hatch spacing, shield gas filed rate, and dwell time, amongst other process variables, can be set to constant values during optimisation [90]. The melt pool dynamics, which are essentially the interactions among the melt pool, powder, and laser beam (MP-P-LB), determine the microstructure, defect formation, dimensional accuracy and surface texture of the deposited part. In a powder system, as the powder particles are supplied from the nozzle, they encounter the laser beam and absorb energy to melt, a process that depends on the available energy density, momentum fields, and the alloy's elemental composition (thermal properties) [91]. The powder size distribution and the angle of incidence on the melt pool also influence the amount of energy absorbed and the resulting melt pool size. A significant amount of powder can be reflected from the melt pool surface if the incident angle is incorrect, and surface tension at the melt pool surface opposes this [92]. Therefore, to optimise process parameters, it is important to fully understand the MP-P-LB interaction, appropriate dendrite arm spacing (PDAS), controlled anisotropy and heat accumulation in deposited layers.

The primary dendrite arm spacing is a microstructural evolution parameter that arises during the solidification of the deposited layer and depends on thermal gradients. Finer dendrite arm spacing is desired for higher strength and hardness and is achieved through high cooling and solidification rates. Slower solidification rates result in coarser spacing, which improves ductility but reduces strength and hardness [93]. Proper optimisation of process parameters, such as laser energy and scan speed, will ensure the desired PDAS. Anisotropy is a mechanical property-dependent condition that results from the direction of the solidification process in the build direction. In LMD and other additive manufacturing processes, grain growth occurs during solidification along the build direction, and the thermal gradient controls the degree of elongation and texture. If the heat-flow direction is inconsistent, it can lead to anisotropic mechanical behaviour, which is detrimental to the mechanical properties of the deposited part [94]. Optimising the laser power and scanning pattern/strategy can significantly enhance the uniformity of thermal flow during solidification by unifying solidification paths and grain orientations. This ensures mechanical isotropy and better mechanical properties. In laser metal deposition and other additive manufacturing processes, heat is not fully dissipated between printed layers. The heat in the previously printed layer does not fully dissipate before the new layer is deposited, thereby raising the new layer's temperature and causing heat accumulation. This accumulated heat promotes the growth of coarse grains and the development of an inhomogeneous microstructure across the deposited part, which can affect its strength, hardness, and ductility [95]. The accumulated heat between deposited layers can also generate residual stresses, leading to warping, cracking, and poor dimensional accuracy [96]. Therefore, to avoid heat accumulation during LMD, it is important to optimise laser power, scan speed, interlayer delay, and scan strategy to enable consistent microstructure growth and mechanical isotropy throughout the build.

4. Experimental Optimisation Techniques

Many studies on parameter optimisation in the LMD process adopted a single-factor experimental method to examine the effect of individual parameters on the quality of the desired material properties [82], [97]. Others employed a multi-objective optimisation technique to determine the impact of two or more parameters on the desired quality and properties of the printed component.

4.1 Single-factor Optimisation

This involves varying the selected value of one process parameter while holding the others constant and performing experiments until the desired outcome is achieved. Ding et al. [82] investigated how laser energy density affects laser cladding of the CoCrFeMnNi HEA. The study varied the laser power, conducting experiments at three selected powers (3200, 3500, and 3800 W) to determine the impact of energy density on the microstructure and wear resistance of cladded coatings. They reported an equiaxed microstructure at 3200 W and a coarse columnar microstructure at 3500 and 3800 W. It reported the best wear resistance at 3500 W, which was the optimal laser power. At 3800 W, wear resistance decreased, resulting in a rougher surface. The findings confirm that moderate energy density (Es) is important for forming a uniform solid solution. However, as Es decreased, there was a tendency toward the formation of amorphous glass microstructures, resulting in weaker adhesion to the substrate. An excessive Es leads to substantial substrate melting, which was detrimental to the alloy's performance. Therefore, energy density must be maintained within an optimal range. Mahamood and his research group [97] examined how laser scan velocity affects the microstructure, hardness, and wear resistance of Ti6Al4V/TiC composites fabricated by LMD. The authors varied the laser scan speed from 0.015 to 0.105 m/s in increments of 0.01 m/s and observed that both microhardness and wear resistance increased with laser scan speed, but beyond 0.065 m/s, wear resistance showed a downward trend. The study also established that at low laser speeds, more TiC melted, whereas at higher speeds, unmelted composites formed, thereby increasing wear resistance. The findings concluded that 0.065 m/s is the optimal scanning speed, above which the microhardness and wear resistance began to decrease. Lee et al. [98] examined the effect of line energy density (LED) on the quality of Ti-6Al-4V produced by LMD. The study printed different samples at laser power levels of 160, 180, 200, and 220 W, respectively, while neglecting the effects of other parameters. Findings revealed that both strength and elongation increased as the LED increased to 12.7 J/mm due to a drop in resultant lack-of-fusion and voids. However, as the LED exceeded 14.11 J/mm, both strength and elongation decreased, giving a useful hint on determining the optimum laser power for LMD of the T64 alloy. Dada et al.[99] found that satelliting AlCoCrFeNiCu and Ti6Al4V powder fractions using double powder feedstock results in a homogeneous microstructure, with a powder feed rate of 2g/min giving surface roughness between 0.5 and 0.80 µm.

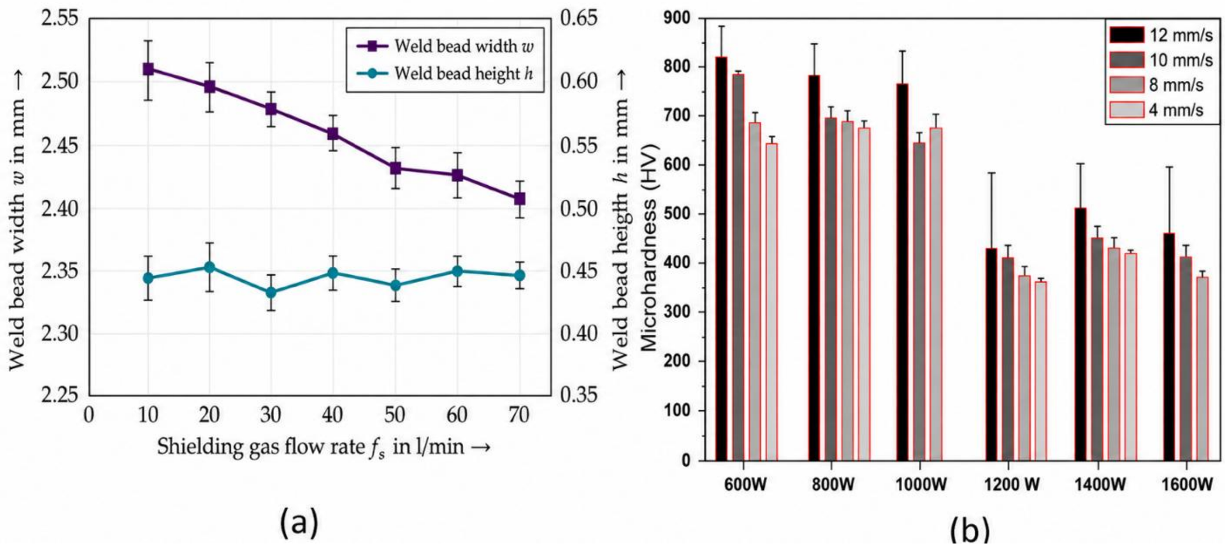

Figure 3. The influence of laser power, laser scan speed, and shield gas field rate on the printed alloys (a) Influence of shield gas flow rate on layer width (ω) and weld height (*h*); the error bars indicate the standard deviations. Reprinted with permission from C. Bernauer et al.[100]; (b) Microhardness of AlTiCrFeCoNi HEA against laser powder [21].

Some researchers varied two parameters to examine their influence on the LMDed product. Hicks et al. [72] studied the effects of laser power and powder feed rate on laser-deposited Ti-5Al-5Mo-5V-3Cr (T-5553). They found that increasing the powder feed rate reduced β-grain size, thereby significantly increasing the microhardness. Bernauer et al. [100] investigated how the novel local shield gas concept affects printing quality in a coaxial wire-feeding LMD using computational simulations. They reported that as the shield gas flow rate increased from 10 to 70 l/min, the melt pool temperature decreased by approximately 10K due to convective cooling, while the bead width and height decreased with increasing flow rate. In a similar study, Dada et al. [21] examined how laser power and scan velocity affect the coatings of the AlCoCrCuFeNi and AlTiCoCrFeNi HEAs. The study employed a design of experiments and optimised deposition outcomes by varying the power between 600 and 1600 W and the laser scan speed between 4 and 12 mm/s, while keeping the gas flow constant at 3 l/min. They also adopted preheating the baseplate as an optimisation tool, heating it to 400 ˚C. The results of their study indicated that the optimal range of laser power and scan velocity for achieving defect-free layers and good hardness in the Ti- and Cu-based HEAs was 1200-1600 W and 8-12 mm/s, respectively, with both alloys showing both FCC and BCC structures. Chen and Zhou [20] manipulated the hatch spacing, laser scan velocity, and laser power to overcome poor mechanical anisotropy and defects in LMD-printed CoCrFeMnNi HEA. The study aimed to suppress coarse columnar grain growth. By holding powder feed rate and hatch spacing constant at approximately 10 g/min and 400 µm, respectively, and observing that, as power increased from 400 to 600 W at a laser scan velocity below 40 mm/s, the cracks were eliminated. The optimum scan velocity of 10 to 30 mm/s and power range of 400 to 600 W yielded defect-free deposits with ultrasonically assisted refined grains of about 14 to 44 µm, and an overall tensile yield strength increased by about 17% without a drop-in ductility. The influence of three parameters (laser power, scanning velocity, and shield gas flow rate), as investigated through single-factor optimisation, on the various printing characteristics is shown in Figure 3. Despite appreciable successes recorded by these studies, optimising a single-factor approach may not be holistic, as it is easier and more accessible. Still, the LMD process is influenced by myriad factors and conditions; controlling only one factor will hardly stabilise the process and achieve the desired, reliable outcome. Therefore, this method is a trial-and-error approach that will be costly if many experiments are required to optimise other parameters. The summary of the optimisation parameters and responses from the single-factor techniques appraised in this study is presented in Table 2.

Table 2. Summary of optimisation parameters and their responses by single-factor methods

No.	Optimisation Process Parameters	Optimum Values	Optimisation Responses	Deposition Method	Deposited Material	Reference
1	Laser power	3500 W	Wear resistance, Refined Microstructure	Laser Cladding	CoCrFeMnNi HEA	[82]
2	Laser scan speed	0.065 m/s	Microstructure, Hardness, Wear resistance	LMD	Ti6Al4V/TiC HEA	[97]
3	Line energy density, Laser power	12.7 J/mm, 200 W	Strength, Ductility	LMD	Ti-6Al-4V	[98]
4	Powder feed Rate, Laser power	2.82 g/min, 3.0 kW	Material utilisation, Width and Height of Deposition, Microstructure, Hardness	LMD	Ti6Al4V	[99]
5	Laser power, Powder feed rate	650 W, 2.3 g/min	Microhardness, Grain refinement	LMD	Ti-5AL-5Mo-5V-3Cr (T-5553	[72]
6	Novel Local Shield gas	40 l/min	Width & height of weld bead	LMD	Austenitic Steel ER316LSi wire	[100]
7	laser power, Scan Speed, Substrate preheating	1200-1600 W, 8-12 mm/s. 400 ºC	High temperature, hardness	LMD	AlCoCrCuFeNi, AlTiCoCrFeNi HEA	[101]
8	Laser power, Scan speed, hatch spacing	400-600 W, 10 – 30 mm/s	Refined Microstructure, Defect-free deposit	LMD	CoCrFeMnNi HEA	[20]

4.2 Response Surface Analysis

Response surface methodology (RSM) is a popular tool for optimising various engineering systems and processes [102], [103]. Researchers used RSM to optimise the LMD of HEAs by determining the effects of parameter combinations. Que et al. [104] optimised microhardness and wear resistance in laser cladded (LC) AlCoCrFeNiTi HEA using RSM. Their results showed that the wear rate increased with laser scanning speed and decreased with increasing laser power and powder feeding voltage. The optimal process parameters for deposition of maximum hardness and minimum wear resistance were 1881 W, 5 mm/s, and a powder feeding voltage of 25 V. Akinwande et al. [105] used a statistical model to predict the laser power and composition of the TiC additive required to improve the microstructure and properties of the CoCrFeMnNi HEA linearly. They reported that increasing TiC content (5-15 wt.%) linearly decreased elongation. Furthermore, laser power increments of 100, 400, and 700 W led to increased microhardness due to the presence of hard TiC inclusions. Their developed models predicted 15% TiC (wt.%) and a laser power of 504 W as the optimal parameters. Jiang et al. [106] adopted RSM to investigate the effects of laser power, laser scan speed, and pulse width on the dilution rate and microhardness during laser deposition of the CoCrFeNiTiAl HEA, utilising ANOVA to analyse the data. Their findings show that laser power and pulse width had a remarkable effect on both dilution rate and microhardness, while pulse width and scanning speed also affected microhardness. The optimum parameters obtained were 676.73 W, 5 mm/s, and 9 ms for power, laser speed, and pulse width, respectively. The relationships between alloy compositions, process parameters, hardness, elongation, and wear volume, as studied with RSM, are depicted in Figure 4. In another development, Dada et al. [101] used a full-factorial DoE to optimise laser power and laser scan velocity via RSM in the LMD of AlTiCrFeCoNi HEA. The RSM was used to validate the results of the analysis of variance (ANOVA). Laser powers of 1500 W and 1600 W, and a scan speed of 10 mm/s were the optimum values, yielding microhardness values up to 450 HV and 715 HV for Ti- and Cu-based HEAs, respectively. Hence, predictive modelling can effectively optimise process parameters during the LMD of HEAs. Huang et al. [107] also employed response surface methodology to optimise the power, scan speed, and powder feed rate during laser cladding, with microhardness, aspect ratio, and dilution rate as output responses. The authors reported that predicted values agree with the actual values within an acceptable 10% error margin. The optimum laser power, scan velocity and powder feed rate were 773.65 W, 5 mm/s, and 15 g/min, respectively, resulting in maximum hardness, aspect ratio, and a 10-20% dilution.

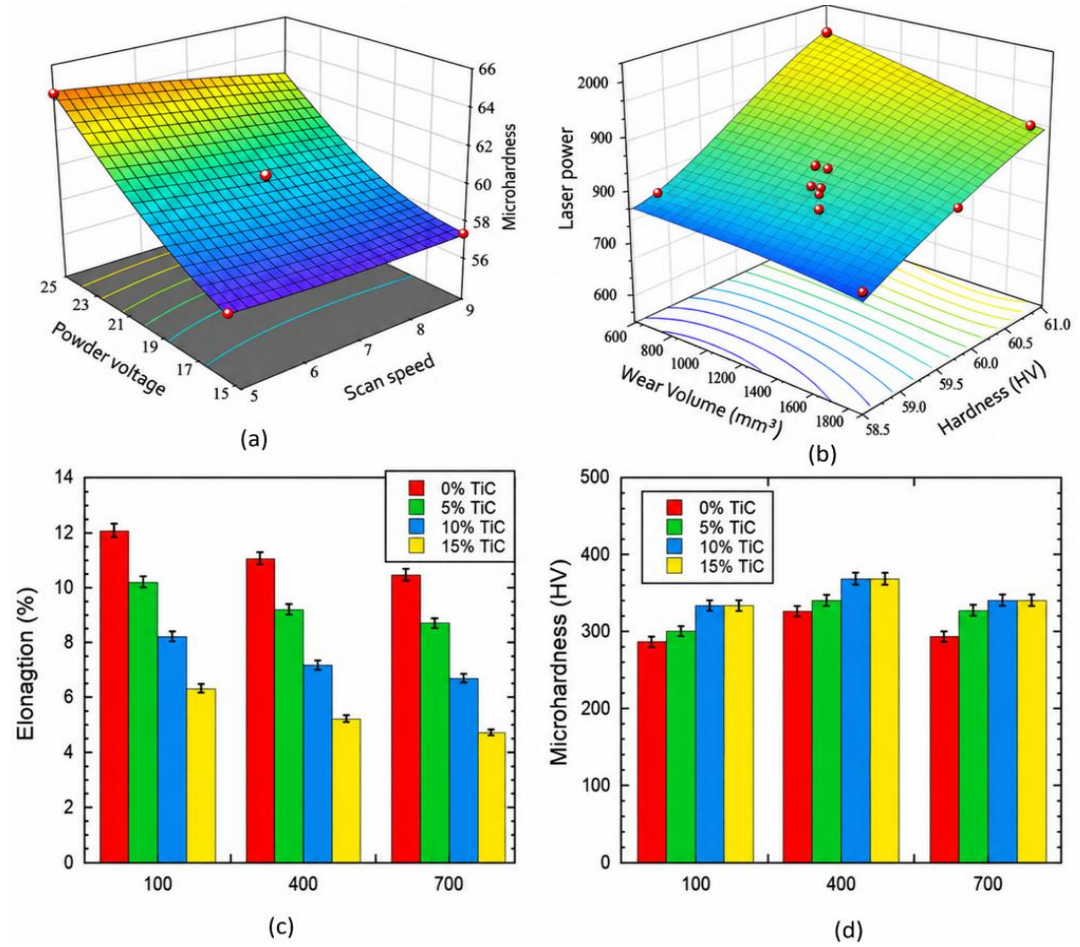

Figure 4. Interaction between process parameters and deposition qualities (a) Relationship between powder feed voltage, scan speed and hardness (b) Influence of laser power on wear volume and hardness; (c) Relationship between TiC dosage and laser power on (c) Elongation; (d) Microhardness [105]

Dong et al. [108] reported that laser power and microhardness were inversely related, while scanning speed and powder feed rate were positively correlated during LMD of $AlCoCrFeNi_{2.1}$EHEA. The study adopted RSM to predict optimum scan speed, laser power, and powder feed rate to maximise microhardness, aspect ratio, and dilution rate responses. The findings reported a high correlation between experimental and predicted results, with an error of 5.27%. The optimal parameters obtained were 1675 W, 7.8 mm/s, and 12.91 g/min, respectively, yielding a microhardness of approximately 322.7 $HV_{0.2}$. Xiao et al. [109] used the same RSM to optimise powder feed rate, scan speed, and laser power for laser cladding of $Ti_3Zr_{1.5}NbVAl_{0.25}$ HEA. The authors obtained a single-track cladding with both equiaxed and columnar microstructures on the inside and grain boundaries, respectively. The optimum parameter values were 1600 W, a scanning speed of 10 mm/s, and a powder feeding rate, with a stable microhardness of 299.99 $HV_{0.2}$ across the melt pool. Still using RSM. Nezhad et al. [103] also studied the effects of powder feed rate, scan speed, and laser power on the geometric features of single-track $Al_{0.5}CoCrFeNiNb_{.0.5}$-$Si_{0.1}$. The predicted and experimental results showed a relative error of 8.55%, and the optimum parameters were 500 W, 4 mm/s, and 106 mg/s, respectively. Duan et al. [110] combined RSM and a non-dominated sorting generalised algorithm (NSGA-II) to optimise LMD of $FeCrNiMo_{0.75}$ HEA. A comparison of their results revealed that the coating's aspect ratio was higher with RSM than with NSGA-II. Additionally, NSGA-II exhibited higher hardness values than RSM optimisation, providing valuable insights for selecting an optimisation method to achieve a specific deposition outcome in practical laser deposition applications for HEAs. The input and output responses optimised using RSM in the reviewed studies are summarised in Table 3. All the reviewed studies achieved varying degrees of success, providing evidence that response surface methodology (RSM) is an effective technique for exploring interactions among multiple process parameters within the tested variables, thereby avoiding the full factorial method, which requires many costly experiments to identify critical and optimal parameters. However, RSM assumes that a polynomial can approximate the relationship between process parameters and response outcomes. This can limit accuracy when dealing with complex compositional systems like HEAs. It is also limited to a relatively small number of variables due to the increasing complexity of statistical models and the cost of experimentation

Table 3. Optimisation Input and Output Response used in Response Surface Methodology

No.	Optimisation Input Parameters	Optimum Values	Optimisation Output Responses	Deposition Method	Deposited Material	Reference
1	Laser power, scan speed, powder feed voltage	1881 W, 5 mm/s, 25 V	Microhardness, wear resistance	LMD	AlCoCrFeNiTi HEA	[104]
2	Laser power, Tic composition	504 W, 15% TiC (wt.%)	Microhardness, porosity	LMD	CoCrFeMnNi HEA	[105]
3	Laser power, scan speed, Pulse width	676.73 W, 5 mm/s, 9 ms	Microhardness, Dilution rate	LMD	CoCrFeNiTiAl HEA	[106]
4	Laser power, scan speed	1500-1600 W, 10 mm/s	Microhardness	LMD	AlTiCrFeCoNi HEA	[101]
5	Laser power, scan speed, Powder feed rate	773.65 W, 5 mm/s, 15 g/min	Aspect ratio, Dilution rate, Microhardness	LMD	CoCrFeCuNi HEA	[107]
6	Laser power, scan speed, Powder feed rate.	1675 W, 7.8 mm/s, 12.91g/min.	Microhardness, Aspect ratio, Dilution rate	LMD	AlCoCrFeNi2.1 HEA	[108]
7	Laser power, scan speed, Powder feed rate	1600 W, 10 mm/s, 1 r/min	Clad width & height, powder efficiency aspect ratio, Microhardness	Laser cladding	$Ti_3Zr_{1.5}NbVAl_{0.25}$ HEA	[109]
8	Laser power, scan speed. Powder feed rate	500 W, 4 mm/s, 106 mg/s	Aspect ratio, Dilution rate, Microhardness	LMD	$Al_{0.5}CoCrFeNiNb._{0.5}$-$Si_{0.1}$ HEA	[103]
9	Laser power, scan Speed, powder feed rate	200-2400 W, 100-150 mm/s, 1.4-1.8 r/min	Microhardness, Aspect ratio	Laser cladding	$FeCrNiMo_{0.75}$ HEA	[110]

4.3 Taguchi Method

Researchers have adopted more robust design-of-experiments approaches, such as the Taguchi method, to optimise key LMD process parameters and achieve desired outcomes, including low porosity, high deposition density, good surface finish, and improved mechanical properties [111], [112]. The Taguchi method uses orthogonal arrays to predict the effects and extent of parameter influence in achieving accurate designs. The method is easy and relatively low-cost, reducing experimental time [113]. Gao et al. [111] optimised the scan speed, power feed rate, laser energy, and substrate tilt angle for 316L stainless steel reinforced with an AlFeCoCrCuNi HEA using the Taguchi method. The study analysed the data using grey regression analysis (GRA). The findings showed that the combination of these parameters significantly affects microhardness, contact angle, and dilution. It reported a high correlation between the predicted and experimental results with only a 0.95% deviation. Optimal parameters that yielded the highest hardness of the deposited coating were determined after 16 experiments to be 11 mm/s, 750 W, and 5 r/min for laser speed, power, and powder feeding rate, respectively. Zhong et al. [114] optimised sputtering deposition parameters in LMD of CoCrFeNi HEA by the Taguchi method. The study findings revealed that the optimised parameters improved the electrical resistance by about 98.2 μΩ·cm, achieved a 0.5 nm improvement in surface texture, and resulted in a hardness of about 9.3 GPa. Kumar and Nair [115] optimised LMD of Ti-6Al-4V alloy using a Taguchi orthogonal design to enhance hardness and bonding strength. The optimised parameter ranges were 2350 to 2650W for laser power, 500 to 700mm/min for scan speed, and 3 to 5g/min for powder feed rate. The optimum values of power, scan velocity, and powder feed rate were 2650 W, 700 mm/min, and 5 g/mm, respectively. The study obtained a maximum hardness of 459.4 HV and a microstructure consisting of an acicular α-phase and a Widmanstätten microstructure. The Taguchi method is less popular than RSM for optimising LMD in HEA systems. This is because, although it requires fewer experiments than a full factorial design, Taguchi's approach has the limitation that it does not provide a predictive model beyond the parameters included in the experiment. Consequently, it may not be ideal for higher-order, nonlinear, and dynamic systems, such as the LMD of complex alloys like HEAs. Hence, researchers adopt more predictive techniques, such as RSM and other predictive models.

4.4 Numerical Simulation

Researchers have also adopted numerical simulations to monitor and optimise engineering systems. To this end, Andi Huang et al. [116] investigated the thermal-fluid dynamics and the microstructure evolution during the LMD of AlCoCrFeNi HEA using a Multiphysics coupling numerical model. The model studied laser-powder interaction and the effects of buoyancy and Marangoni convection on the melt pool. Their results reveal strong bidirectional coupling between temperature and the flow field, with Marangoni convection as the primary heat-transfer mechanism. Kanyane et al. [117] sought to overcome low hardness by simulating the cladding of Ti-6Al-4V with an AlCrNiTiNb HEA, using COSMOX Multiphysics to analyse the temperature distribution in the deposited layers. The study found that increasing laser energy from 1150 to 1350 W affected the dimensions of the melt pool, the solidification rate, and the microstructural formations in the deposited HEA coating. It also recorded a significant increase in microhardness from 314 to 892 HV at a laser power of 1350 W, due to a solid solution composed of BCC and FCC phases. Modupeola et al. [7] optimised process parameters for LMD of HEA on A301 steel using COSMOL/Multiphysics to simulate the alloy's temperature distribution. Using an extra-fine mesh in the domain where the laser moved resulted in good model accuracy, and the Gaussian profile indicated that the base plate had an adequate surface temperature to improve adhesion and reduce thermal stresses, thereby yielding optimal HEA deposition. Chen [118] adopted the least squares method to determine the effect of heat energy on the width, height, and dilution ratio of laser-clad CrMnFeCoNi HEA coatings. The fitted linear equation for heat input and coating geometry indicates that higher heat input leads to a more uniform element distribution; this effect was observed at heat inputs above 2 J/mm. Gao et al. [119] applied a numerical gas-powder flow model to study the effect of powder feeding on density and surface texture in laser metal deposition. The study found that the optimal powder flow rate was 2.5-3.5 kg/h and the gas flow rate was 6 L/min, which resulted in high deposition density and efficient powder utilisation. Numerical simulation has enabled understanding of complex physical processes, such as solidification behaviour, melt pool dynamics, and temperature gradients, which are difficult to observe experimentally. These processes are crucial for understanding both phase and microstructure evolution. However, the multiprincipal nature of HEAs complicates phase prediction and thermodynamic modelling, requiring reliable thermophysical property data and substantial expertise.

4.5 Statistical Methods

Researchers have used traditional statistical approaches, such as regression analysis (RA) and analysis of variance (ANOVA), to investigate the impact of process parameters on the quality of deposits/claddings [120], [121]. The regression analysis is invaluable for optimising the LMD of HEAs, as it quantitatively analyses the correlations between process parameters and expected performance qualities, enabling the design of high-performance alloys based on optimally predicted parameters. Xue et al. [120] used ANOVA in validating the optimised response surface model parameters for laser metal deposition of a CrCoNi medium-entropy alloy. Their analysis yielded optimal values of 750.343 W, 9.530 mm/s, and 1.870 r/min for power, scan velocity, and powder flow rate, respectively. Their findings showed that as power increased, the melt pool size increased, while porosity decreased. ANOVA regression analysis was also used by Dada et al. [101] to assess the influence of LMD parameters on hardness during the fabrication of the AlCrCoFeNiTi HEA. In the study, both laser power and scanning velocity were significant in the LMD of the AlCoCrFeNiTi HEA, and hardness increased with higher values of both parameters. Thus, increasing power and scanning speed improves mechanical properties, and the increased hardness is due to the high solidification rate of LMD. Gao [122] used a single-factor ANOVA to validate the RSM-predicted effect of parameters on hardness, porosity, and dilution rate in laser cladding of the MoNbTiZr refractory high-entropy alloy (RHEA), thereby eliminating insignificant factors. Surprisingly, their findings indicated that powder feeding rate and laser speed contribute more significantly to deposition accuracy, with a stronger influence on porosity, as evidenced by their high F-values. In a similar study, Siddiqui et al. [123] employed ANOVA to validate the RSM-predicted parameters by eliminating insignificant factors in the laser cladding of $AlCu_{0.5}FeNiTi$ HEA. Their ANOVA results indicated that laser power, velocity, and powder feeding rate each strongly contribute to the dilution rate of clad coatings. Huang et al. [107] validated the RSM responses by assessing the significance of the impact factors using F-values. The analysis showed that laser scan speed had the greatest impact on aspect ratio, before energy density and powder flow rate. Akinwande et al. [105] established the significance of input variables of TiC dosage and power on density and pore formation in CoCrFeMnNi)100 –x/TiCx HEA printed by LMD. Analysis of the results indicates that TiC dosage and laser energy had the greatest influence on porosity and density.

Ansari et al. [124], with the aid of regression analysis (RA), established that the clad characteristics (width, height, dilution rate, penetration depth and aspect ratio) of laser-cladded NiCrAlY HEA alloy were affected by the combined parameters ($P^{\alpha}V^{\beta}F^{\gamma}$). The study established that high power and powder flow rate, as well as low scan velocity, increased deposition height and width. Conventional statistical optimisation methods are often focused on a given process. They hardly identify significant factors such as cooling and solidification rates, which are not included in the experiment, necessitating more extensive experiments to numerically simulate the temperature field. Also, microstructural heterogeneity in HEAs and machine fluctuations can introduce noise that affects ANOVA results, especially in laser additive processes such as LMD. In addition, most traditional statistical regression models struggle to handle the increasing complexity of the factors common to HEAs. As the number of process factors and levels increases, the design matrix can become enormous and complex to control.

4.6 Machine Learning Techniques

The use of machine learning (ML) has revolutionised process optimisation in laser additive manufacturing (LAM), enabling not only parameter optimisation but also predictive modelling [125], [126]. In laser metal deposition, machine learning (ML) has enabled accurate control over bead geometry, microstructure, and mechanical properties. It has enabled industries to create models that predict layer heights within milliseconds, enabling dynamic parameter adjustments during laser deposition [127], [128]. Zhang et al. [129] combined Non-Dominated Sorting Genetic Algorithm (NSGA-II) and Generalised Regression Neural Network (GRNN) to optimise laser energy, scanning velocity and powder feeding rate to achieve optimal rate of dilution, aspect ratio, and heat-affected zone (HAZ) in laser-clad CoCrFeNiMn HEA. Both GRNN optimisation and NSGA-II achieved a 10% reduction in error between experimental and predicted results. Optimum parameters resulted in dense laser cladding with no cracks or porosity and improved surface hardness. Researchers have also demonstrated that machine learning can be used to optimise the design of the composition of laser-deposited corrosion-resistant HEA coatings by adjusting input parameters, including composition ratios and process parameters [130]. In related work, Lin et al.[131] designed a hard and wear-resistant FeCrTiMoxSiy HEA coating using a combination of several ML models, including Support Vector Machine (SVM), eXtreme Gradient Boost (XGBoost), and Artificial Neural Network (ANN). In a Python environment, SVM showed the best phase structure and hardness, achieving accuracy, precision, recall, and F1 score values of 0.88. Diwkar et al. [132] studied the metallurgical bonding of an FeCoNiCrMo HEA coating on EN24, using a combination of ML models, including SVM, K-Nearest Neighbour (KNN), and Multilayer Perceptron (MLP). Based on R^2 values, the KNN model achieved the highest accuracy, with an R^2 of 1 across all responses (clad width, height, depth, heat penetration, and microhardness), indicating the best fit to the substrate. In a similar study, Hosseni [133] optimised the hardness of Nb-Ti-V-Zr RHEA by several ML models to train 66 atomic and phase features that affect the hardness of the deposited HEA. The Support Vector Regression showed the best prediction among other models, indicating that as atomic size (d) and configurational entropy (ΔS_{mix}) increase, hardness also increases, confirming their strong influence on hardness.

Brooke et al. [23] used a combination of multilinear regression (MLR) and ANN models to study layer height and grain size, using laser power, laser scan speed, and laser spot size as input variables. The study observed a smaller error margin in ANN results, achieving an R^2 of 0.97 and a root mean square error of 9.68 μm, compared with the MLR model. Asad et al. [134] also obtained a consistently superior (R^2) with ANN, which was better than the regression model by about 44.38%. Machine learning was also used by Sivaraman et al. [135] to predict the wear rate and phase composition of HEAs by training ML models on phase and wear parameters from HEA coatings, including XGBoost, SVM-RBT, ANN, RF, GNB, and logistic regression. XGBoost demonstrated better predictive performance, with an R^2 value of 0.98, showing the lowest error between predicted and experimental values. On the contrary, the RF model achieved the highest phase prediction precision, at about 98.5%. This serves as a guide to the development of AlBeSiTiV HEA coatings for industrial applications. Liu et al. [136] further demonstrated the use of ML algorithms for phase prediction in laser-clad HEA coatings, using dilution rate and carbon equivalent as input parameters. Results of the Shapley Additional Explanation (SHAP) model show that valence electron concentration (VEC) is the dominant factor in phase stability. Optimum parameters obtained for forming stable BCC phase, FCC phase and dual-phase (BCC+FCC) structures were (VEC < 7.4, atomic size, d < 7.63 μm), (VEC > 7.5, atomic size, d < 7.46 μm) and (VEC 7.2-7.8 and atomic size, d 2.5 μm-8.24μm), respectively. Sachin et al. [137] employed TOPSIS to optimise the weight proportion of groundnut shell (GNS) in the manufacture of shell-fibre-reinforced polymer composite. The study obtained an optimal value of 30 wt.% to maximise the desired mechanical properties. Gao et al. [119] used a neural network machine learning algorithm to study the process parameters for LMD of NiTi alloy, maximising material responses by optimising them using NSGA-II. The study obtained an optimal power of 1282 W, a scanning velocity of 8.79 mm/s and a powder feeding of 16 g/min. Additionally, significant improvements in the deposited material (hardness: 267.14 (5.23%) and roughness: 7.86 μm (20.04%) were obtained. Chen et al. [22] also used NSGA-II to analyse the RSM-predicted power, scanning velocity, and powder feeding rate to optimise material outcomes (shape coefficient, dilution, and wetting angle) in laser direct energy deposition (LDED) of CoCrFeNi HEA. Shang et al. [138] adopted the accurate inverse optimisation framework for direct energy deposition (AIDED) machine learning (ML) to predict single-track and multi-track data, achieving accuracy of 0.995 and 0.966, respectively.

Machine learning has been used to develop online process control models that regulate process variables in real time to mitigate over-deposition and improve the quality of the produced parts [126], [128]. To this end, Perani and et al. [139] designed a Long Short-Term Memory (LSTM) Neural Network (NN) for reducing over-deposition in laser metal deposition (LMD) on Inconel 718 alloy, predicting the deposited height of complex random tracks with minimum process loss, demonstrating the use of machine learning for optimising cold spray processes. Hamrani et al. [140] adopted a two-stage ML approach to optimise deposit efficiency in a cold-spray process, and the results indicated that the type and temperature of the gas are the main parameters controlling deposition efficiency. Hydrogen gas was the most cost-effective alternative for deposition, ahead of helium and nitrogen. They also reported that the optimum parameters were Gas type (air, nitrogen, helium, and hydrogen), gas temperature range (100 to 800 ^{o}C), gas pressure (5 to 60 bar), and nozzle configuration diameters of 15, 1.75, and 2mm. The optimum process parameters were 441 W, 6.57 mm/s, and 0.85% for the powder, scanning velocity, and powder flow rate, respectively. Other machine learning and traditional optimisation techniques, such as support vector machines (SVMs) and particle swarm optimisation, have also been adopted by researchers in recent times to improve convergence in multi-objective optimisation for deposition/cladding. The PSO algorithm considers variables as a group rather than as single individuals, as in the case of GA [141].

Table 4. Classification of reviewed studies on machine learning for optimisation in additive manufacturing

S/N	Research Field	ML Technology	Input Variables to Optimise	Response/ Research Target	Reference
1	Optimising Process Parameters	GRNN, NSGA-II	Power (W), scan velocity (mm/s), powder feed rate (g/min)	Aspect ratio, dilution rate, and heat-affected zone	[129]
2	Quality Optimisation	ANN, MLR	Power(W), scan velocity (mm/min), spot Size (mm), global energy distribution, (J/mm^2)	Grain size (μm), Layer height (mm)	[23]
3	Quality Optimisation	SVM & XGBoost	VEC and ΔH_{mix}	Phase structure hardness	[131]
4	Quality Optimisation	ANN	Homogenisation annealing temperature (°C)	Dispersoids and grain boundary strengthening	[142]
5	Quality & Parameters Optimisation	KNN, MLP	Power, scan velocity, powder feeding rate	Depth-of-heat penetration, clad height, microhardness	[132]
6	Quality Optimisation	SVR	atomic size difference (δ), configurational entropy of mixture ($\Delta Smix$), average deviation of electronegativity (AdE)	Hardness	[133]
7	Quality & Parameters Optimisation	XGBoost, SVM-RBT, ANN, RF, GNB	VEC, atomic size (δ), ΔHmix, ΔSmix	Wear rate, and phase formation	[135]
8	Quality Prediction	BPNN	Power(W), scan velocity (mm/s), powder feed rate (g/min)	Microhardness, roughness, and deposit rate	[119]
9	Defect Detection	LSTM	Power, scan velocity, intensity of image (I_{mean})	Deposited Height	[139]
10	Efficiency and Parameters Optimisation	ML-IAM	Gas Temperature, Gas Type	Deposition efficiency	[140]
11	Quality Prediction	PSO, GA	Material (%), power (W), hatch distance (mm), Scan (mm/s), layer distance (mm)	Density	[25]
12	Quality & Parameters Optimisation	PSO, ANN	Power (KW), scan velocity peed (m/s), powder flow rate (rpm), material (%)	Wear volume (mm^3)	[24]
13	Quality Prediction	DL, ML	Power(W), powder feed rate (g/min), density (g/cm3), material (%)	Hardness (top), (middle) and (bottom)	[143]
14	Parameter Optimisation, Quality Prediction	VSM	Wire feed speed, torch angle	Bead central angle	[127]
15	Quality Prediction, DE	M-SVR	Power, Scan velocity, Powder feed rate	Layer width and height	[26]

To this end, Murat et al. [25] employed particle swarm optimisation (PSO) and genetic algorithm (GA) models to predict the optimum parameters for maximum tensile strength in selective laser melting (SLM) of Ti6Al4V alloy without many experiments, which predicted a laser power of 100 W and a scanning speed of 719 mm/s for maximum tensile strength. The results show that PSO-based prediction was more accurate than GA-based prediction. Ngwoke et al. [24] explored both PSO and ANN to determine optimal parameters for the LMD of Ti-6Al-4V to improve deposition efficiency and minimise experimental costs. Wong et al. [143] predicted deposition outcomes in bimetallic tracks produced by DED using an SVM. The study obtained a very good fit. The loss convergence and loss function are 150 and 80% bead accuracy. Kim et al. [127] introduced the SVM algorithm in Wire-Arc Additive Manufacturing (WAAM) to optimise bead geometry by defining optimal deposit conditions, and the predicted conditions were accurate. Chen and fellow researchers [26] developed a Multi-output Support Vector Regression (M-SVR) algorithm to predict optimal layer width and height for maximum performance. The findings revealed a 22% reduction in root mean square error and a 5.5% reduction in absolute error compared to the single-output SVR and Backpropagation Neural Network (BPNN), respectively. As evidenced by the reviewed studies, neural networks are effective for handling large-scale data scenarios such as LMD of HEAs. However, larger data samples can pose challenges for accurate training and may require longer training times. For this reason, researchers have been combining neural networks with other optimisation algorithms [129] . The genetic algorithm is an improvement on traditional optimisation models that rely on random search techniques. Researchers use it in combination with neural networks for faster global optimisation. Its advantage lies in its worldwide search capability and its ability to handle nonlinear and multi-variable cases, such as in LMD. However, the slow convergence and high computational demand underscore the need for a hybrid approach that combines GA with other ML models [25]. It is an extremely intelligent model that has been utilised for LMD of HEAs due to its predictive power and performance in regression and classification compared to other algorithms. XGBoost is another model that performs well, but it lacks the inherent temporal modelling capabilities to simulate time-dependent processes, such as melt pool evolution, except when combined with other physical models. Particle swarm optimisation (PSO) is another global search algorithm that is particularly well-suited to problems with fewer variables for accurate convergence. It has been employed in the LMD of HEAs due to their complex, nonlinear relationships. Despite its fast convergence, PSO may get trapped in local optima in a multimodal system such as HEA processing and fail to converge. The support vector machine is another effective machine learning model that can be trained on smaller datasets. Although it takes a very long time to converge with large data, the accuracy can be poor. The SVM model can be trained more accurately with fewer data. However, it is a regression model and cannot be optimised on its own, except when used with other optimisation methods, such as PSO. It is evident from the reviewed studies that machine learning algorithms are increasingly employed in laser metal deposition and cladding of HEAs despite the challenges encountered. More accurate predictive performance through intelligent algorithms will require models that can handle high-dimensional data, mitigate overfitting, and maintain computational efficiency. This demands much experimentation and data training, which is costly as well. Critically examining all the reviewed studies, none relied on a single algorithm to obtain optimal parameters or predictions, thereby avoiding local convergence. The summary of the intelligent algorithm-optimised variables and responses is shown in Table 4.

5. Conclusions

This review study systematically examined the defects associated with the LMD of HEAs, including the governing process parameters, and the optimisation strategies for minimising the defects. The optimisation of the LMD of HEAs remains a difficult task due to the multiple variables involved, 13 of which are critical to the microstructural evolution and mechanical performance of the part. The reviewed studies show that the right control of key processing parameters such as laser power, scan speed, powder feed rate, layer thickness, shield gas flow rate, and overlap fraction can remarkably decrease associated defects, cracks, porosity, lack of fusion, and impurities, as well as improve hardness, wear resistance and microstructural homogeneity. Quantitative evidence from reviewed studies indicates that optimised parameter ranges of 400-1600 W, 5-30 mm/s, and 1-16 g/min deliver defect-free HEA deposits, with hardness values between 322 and 715 HV and a highly refined microstructure down to a dendrite arm spacing of 1.14μm. Innovative optimisation methods such as Taguchi, response surface methodology, numerical simulation, and machine learning techniques achieved high prediction accuracy, with R^2 values close to 1.0. Good wear-rate prediction within 5-10% error and defect-detection accuracy of about 90% were achieved. The reviewed studies further establish that hybrid optimisation techniques, which merge two or more machine learning algorithms, achieve higher predictive accuracy. It can be concluded from the findings that combining machine learning techniques with physics-based modelling and digital twin models is the best approach for fabricating defect-free and high-quality HEA parts through LMD, delivering accessible groundwork for commercial-scale applications and future research in additive manufacturing of HEAs

The LMD process has defects like cracks, lack of fusion, porosity, impurities, and surface-connected porosity. Understanding these helps improve control, reduce defects, and enhance part quality. Optimising parameters in LMD of HEAs is vital but complex due to their multi-element nature. Researchers have used various techniques, starting with single-factor optimisation. Later, Taguchi, RSM, numerical simulations, and other statistical methods for multi-objective optimisation were adopted. While numerical simulations have limitations, computer-aided machine learning has enabled more intelligent optimisation algorithms. Despite some success, machine learning approaches face issues such as long convergence times and limited predictive accuracy, with each method having its own limitations. Recent research shows that combining multiple machine learning techniques yields better results. As research on LMD-fabricated HEAs progresses, many believe that developments in machine learning will follow suit. Many hybrid intelligent algorithms have enabled a transformative approach to process optimisation in the LMD of HEAs, facilitating faster, more accurate, and more adaptive manufacturing. However, accuracy will depend on data quality, integration infrastructure, and interpretability. Future work should focus on developing hybrid techniques that combine data-driven algorithms, physics-based simulations, and experimental validation to achieve robust solutions with generalisable outputs for LMD of HEAs. Researchers believe that future optimisation of LMDed HEAs should focus on developing novel digital twin algorithms that integrate real-time sensor data to simulate and enable in situ control of the LMD process. These can predict temperature profiles and optimise laser parameters in real time to improve the evolution of the microstructure and the mechanical properties of the deposited HEAs. Integrating real-time monitoring tools, such as cameras and spectrometers, into modelling systems will enable observation of the LMD process in real time. This will enable detection of anomalies and melt-pool dynamics, providing timely feedback for process adjustments and ensuring reliable, consistent HEA deposition. These forward-looking strategies for improving machine learning algorithms aim to transform the LMD of HEAs, making the process more adaptable, efficient, and capable of producing tailored-property HEAs for advanced engineering applications.

Acknowledgements

The authors acknowledge the Ministry of Higher Education for funding this research. Many thanks also to the Universiti Teknologi Malaysia (UTM) for facilitating the grant and for providing an enabling environment for the study.

Funding

This study is funded by the Ministry of Higher Education of Malaysia through the Fundamental Research Grant Scheme (FRGS), No: FRGS/1/2022/TK10/UTM/02/45.

Conflict of Interest Declaration
The authors declare no conflict of interest with respect to this study.

CRediT Authorship Contribution Statement
Agbaye Ignatius Uyabemem: Conceptualisation; Methodology; Writing original draft
Aini Zuhra Abdul Kadir: Conceptualisation; Investigation; Validation; Supervisor; Writing- revise & review
Tuty Asma Abu Bakar: Conceptualisation; Data acquisition; Analysis; Project administration; Supervisor; Writing- revise & review

Availability of Data and Materials
This is a review study, and all sourced materials and findings are available on request from the corresponding author.

Ethics Declaration
This study is a review work and has nothing to do with human or animal participants. Therefore, ethical approval was not necessary.

Generative Artificial Intelligence Declaration
The authors declare that no artificial intelligence-assisted technologies were used to generate ideas or theories in this work, except to enhance the readability of the figures and language. It was used with careful human control and regulation. The authors take full responsibility for the content

References

[1] B. Cantor, I. T. H. Chang, P. Knight, A. J. B. Vincent, "Microstructural development in equiatomic multicomponent alloys," *Materials Science and Engineering: A*, vol. 375–377, no. 1-2 SPEC. ISS., pp. 213–218 2004. https://doi.10.1016/j.msea.2003.10.257

[2] J.W. Yeh, S.K. Chen, S.J. Lin, J.Y. Gan, T.S. Chin, T.T. Shun et al., "Nanostructured high-entropy alloys with multiple principal elements: Novel alloy design concepts and outcomes," *Advanced Engineering Materials*, vol. 6, no. 5, pp. 299–303, 2004. https://doi.org/10.1002/adem.200300567

[3] Z. Wang, S. Zhang, "Research and Application Progress of High-Entropy Alloys," Nov. 2023, *Multidisciplinary Digital Publishing Institute (MDPI)*. https://doi: 10.3390/coatings13111916

[4] H. Song, F. Tian, Q.M. Hu, L. Vitos, Y. Wang, J. Shen et al. "Local lattice distortion in high-entropy alloys," *Physical Review Material*, vol. 1, no. 2, p. 023404, 2017. https://doi.org/10.1103/PhysRevMaterials.1.023404

[5] R. Wang, Y. Tang, S. Li, Y. Ai, Y. Li, B. Xiao, et al., "Effect of lattice distortion on the diffusion behavior of high-entropy alloys," Journal of Alloys Compound, vol. 825, p. 154099, 2020. https://doi.org/10.1016/j.jallcom.2020.154099

[6] A. Mehta,Y. Sohn, "High Entropy and Sluggish Diffusion "core" Effects in Senary FCC Al-Co-Cr-Fe-Ni-Mn Alloys', *ACS Combinatorial Science.*, vol. 22, no. 12, pp. 757–767, 2020. https://doi.10.1021/acscombsci.0c00096

[7] D. Modupeola, P. Patricia, "Optimizing the maximum strain of a laser-deposited high-entropy alloy using COMSOL Multiphysics," *Beni. Suef. University Journal of Basic Applied Sciences*, vol. 13, no. 1,2024. https://doi.10.1186/s43088-024-00542-5

[8] H. Pan, Y. Yuan, Y. Yang, Z. He, S. Jiang, M. Zhu et al., "Multi-scaled heterostructure enables superior strength–ductility combination of a CoCrFeMnN compositionally-complex alloy," *Journal of Material Science Technology*, vol. 222, pp. 82–93, 2025. https://doi.org/10.1016/j.jmst.2024.10.015

[9] T. Lindner, M. Löbel, B. Sattler, T. Lampke, "Surface hardening of FCC phase high-entropy alloy system by powder-pack boriding," *Surface Coating Technology*, vol. 371, pp. 389–394, 2019. https://doi.10.1016/j.surfcoat.2018.10.017

[10] M. Arshad, S. Bano, M. Amer, V. Janik, Q. Hayat, M. Bai, "High-Temperature Oxidation and Phase Stability of AlCrCoFeNi High Entropy Alloy: Insights from In Situ HT-XRD and Thermodynamic Calculations," *Materials*, vol. 17, no. 14,2024. https://doi.10.3390/ma17143579

[11] X. Li, J. Yuan, K. Lu, K. Chong, L. Liu, Z. Zhang, et al., "Corrosion resistance and passive film stability of laser direct energy deposited TiVZrNbAl lightweight multi-principal element alloy," *Corrosion Science*. vol. 239, 2024. https://doi.org/10.1016/j.corsci.2024.112391

[12] M. Wang, Y. Lu, J. Lan, T. Wang, C. Zhang, Z. Cao et al., "Lightweight, ultrastrong and high thermal-stable eutectic high-entropy alloys for elevated-temperature applications," *Acta Materialia*, vol. 248, p. 118816, 2023. https://doi.org/10.1016/j.actamat.2023.118806

[13] Z. U. Arif, M. Y. Khalid, A. Al Rashid, E. ur Rehman, M. Atif, "Laser deposition of high-entropy alloys: A comprehensive review," 2022, *Elsevier Ltd*. doi: 10.1016/j.optlastec.2021.107447

[14] N. Shamsaei, A. Yadollahi, L. Bian, S. M. Thompson, "An overview of Direct Laser Deposition for additive manufacturing; Part II: Mechanical behavior, process parameter optimization and control," 2015. *Elsevier B.V.* https://doi.10.1016/j.addma.2015.07.002

[15] C. Zhong, T. Biermann, A. Gasser, R. Poprawe, "Experimental study of effects of main process parameters on porosity, track geometry, deposition rate, and powder efficiency for high deposition rate laser metal deposition," *Journal of Laser Applications*, vol. 27, no. 4,2015. https://doi.10.2351/1.4923335

[16] Z. Chen, W. Zhu, H. Wang, Q. He, Q. Fang, X. Liu et al., "Overcoming strength-toughness trade-off in a eutectic high entropy alloy by optimizing chemical and microstructural heterogeneities," *Communication Material*, vol. 5, no. 1, p. 12, 2024. https://doi.org/10.1038/s43246-024-00450-2

[17] M. Liu, A. Kumar, S. Bukkapatnam, M. Kuttolamadom, "A review of the anomalies in directed energy deposition (DED) processes & potential solutions - Part quality & defects," in *Procedia Manufacturing*, Elsevier B.V., 2021, pp. 507–518. https://doi.10.1016/j.promfg.2021.06.093

[18] A. Das, D. Ghosh, S. F. Lau, P. Srivastava, A. Ghosh, C. F. Ding, "A critical review of process monitoring for laser-based additive manufacturing," 2024. *Elsevier Ltd*. https://doi.10.1016/j.aei.2024.102932

[19] B. Chen, Y. Zhao, H. Yang, J. Zhao, "Process Parameters Optimization and Numerical Simulation of AlCoCrFeNi High-Entropy Alloy Coating via Laser Cladding," *Materials*, vol. 17, no. 17,2024. https://doi.10.3390/ma17174243

[20] Y. Chen, Q. Zhou, "Directed energy deposition additive manufacturing of CoCrFeMnNi high-entropy alloy towards densification, grain structure control and improved tensile properties," *Materials Science and Engineering: A*, vol. 860, 2022. https://doi.10.1016/j.msea.2022.144272

[21] M. Dada, P. Popoola, N. Mathe, S. Pityana, S. Adeosun, O. Aramide, et al., "Process optimization of high entropy alloys by laser additive manufacturing," *Engineering Reports*, vol. 2, no. 10, p. e12252, 2020. https://doi.org/10.1002/eng2.12252

[22] Y. Chen, C. Guan, J. Li, F. Meng, C. Zhang, X. Wang et al., "Analysis and prediction of morphology and properties of laser-directed energy deposition CoCrFeNi high-entropy alloy using response surface methodology and non-dominated sorting genetic Algorithm II," *Journal of Material Engineering Performance*, vol. 34, no. 12, pp. 11791–803, 2025. https://doi.org/10.1007/s11665-024-09985-4

[23] R. Brooke, D. Qiu, T. Le, M. A. Gibson, D. Zhang, M. Easton, "Optimising the manufacturing of a β-Ti alloy produced via direct energy deposition using small dataset machine learning," *Science Report*, vol. 14, no. 1, Dec. 2024, https://doi.10.1038/s41598-024-57498-w

[24] C. C. Ngwoke, R. M. Mahamood, V. S. Aigbodion, T. C. Jen, P. A. Adedeji, E. T. Akinlabi, "Soft computing-based process optimization in laser metal deposition of Ti-6Al-4 V," *International Journal of Advanced Manufacturing Technology*, vol. 120, no. 1–2, pp. 1079–1093, 2022. https://doi.10.1007/s00170-022-08781-5

[25] F. Murat, İ. Kaymaz, A. T. Şensoy, İ. H. Korkmaz, "Determining the Optimum Process Parameters of Selective Laser Melting via Particle Swarm Optimization Based on the Response Surface Method," *Metals and Materials International*, vol. 29, no. 1, pp. 59–70, 2023, https://doi.10.1007/s12540-022-01205-9

[26] X. Chen, M. Xiao, D. Kang, Y. Sang, Z. Zhang, X. Jin, "Prediction of geometric characteristics of melt track based on direct laser deposition using m-svr algorithm," *Materials*, vol. 14, no. 23, 2021. https://doi.10.3390/ma14237221

[27] C. Guo, G. Li, S. Li, X. Hu, H. Lu, X. Li et al., "Additive manufacturing of Ni-based superalloys: Residual stress, mechanisms of crack formation and strategies for crack inhibition*,*" *Nano Materials Science*, vol. 5, p. 53–77, 2023. https://doi.org/10.1016/j.nanoms.2022.08.001

[28] X. Cao, S. Tian, F. Xu, G. Zhang, "Research on hot cracking in laser welding of Al-contaminated CoCrFeMnNi high-entropy alloys," *Heliyon*, vol. 10, no. 16, 2024. https://doi.10.1016/j.heliyon.2024.e36492

[29] J. Platl, S. Bodner, C. Hofer, A. Landefeld, H. Leitner, C. Turk et al., "Cracking mechanism in a laser powder bed fused cold-work tool steel: The role of residual stresses, microstructure and local elemental concentrations," *Acta Materialia,* vol. 225, p. 117570, 2022. https://doi.org/10.1016/j.actamat.2021.117570

[30] B. Cui, W. Liu, H. Bian, K. Q. Chen, X. Xu, "Investigation of the influence of process parameters on crack formation and mechanisms in Ti-48Al-2Cr-2Nb alloy via laser directed energy deposition," *Material Research Express*, vol. 10, no. 12, 2023. https://doi.10.1088/2053-1591/ad14c3

[31] W. Li, F. Qian, J. Li, Y. Zhu, Y. Liang, S. Xu et al., "Design strategy for eliminating cracking and improving mechanical properties of Al-Mg-Si alloys fabricated by laser melting deposition," *Additive Manufacturing*, vol. 68, p. 103513, 2023. https://doi.org/10.1016/j.addma.2023.103513

[32] J. Yu, M. Rombouts, G. Maes, "Cracking behavior and mechanical properties of austenitic stainless steel parts produced by laser metal deposition," *Materials and Design*, vol. 45, pp. 228–235, 2013, https://doi.10.1016/j.matdes.2012.08.078

[33] F. Soffel, K. Papis, M. Bambach, K. Wegener, "Laser Preheating for Hot Crack Reduction in Direct Metal Deposition of Inconel 738LC," *Metals (Basel).*, vol. 12, no. 4, 2022. https://doi.10.3390/met12040614

[34] M. C. Brennan, J. S. Keist, T. A. Palmer, "Defects in Metal Additive Manufacturing Processes," *Journal of Materials Engineering and Performance*, vol. 30, no. 7, pp. 4808–4818, 2021. https://doi.10.1007/s11665-021-05919-6

[35] V. Ingle, M. Sorte, "Defects, Root Causes in Casting Process and Their Remedies: Review," *International Journal of Engineering Research and Applications*, vol. 07, no. 03, pp. 47–54, 2017. https://doi.10.9790/9622-0703034754

[36] X. Bi, R. Li, T. Li, X. Zhang, J. Cheng, Y. Tian, "Cracks suppression strategies for CoCrNi medium entropy alloy fabricated by laser directed energy deposition," *Material and Design*, vol. 226, 2023, https://doi.10.1016/j.matdes.2022.111579

[37] Q. Guo, S. Chen, M. Wei, J. Liang, C. Liu, M. Wang, "Formation and Elimination Mechanism of Lack of Fusion and Cracks in Direct Laser Deposition 24CrNiMoY Alloy Steel," *Journal of Materials Engineering and Performance*, vol. 29, no. 10, pp. 6439–6454, 2020. https://doi.10.1007/s11665-020-05163-4

[38] S. Mojumder, Z. Gan, Y. Li, A. Al Amin, W. K. Liu, "Linking process parameters with lack-of-fusion porosity for laser powder bed fusion metal additive manufacturing," *Additive Manufacturing*, vol. 68,2023. https://doi.10.1016/j.addma.2023.103500

[39] R. Savinov, Y. Wang, J. Wang, J. Shi, "Comparison of microstructure and properties of CoCrFeMnNi high-entropy alloy from selective laser melting and directed energy deposition processes," in *Procedia Manufacturing*, Elsevier B.V., 2021, pp. 435–442. https://doi.10.1016/j.promfg.2021.06.046

[40] Z. Gao, D. Li, Y. Zhao, C. He, H. Lin, "Microstructure and Mechanical Properties of TiB2/AlSi10Mg Composites Fabricated by Laser Metal Deposition," *JOM*, vol. 77, no. 4, pp. 2392–2404, 2025. https://doi.10.1007/s11837-025-07171-y

[41] F. Bruzzo, G. Catalano, A. G. Demir, B. Previtali, "In-process laser re-melting of thin walled parts to improve surface quality after laser metal deposition," in *Key Engineering Materials*, Trans Tech Publications Ltd, 2019, pp. 191–196. https://doi.10.4028/www.scientific.net/KEM.813.191

[42] H. Dobbelstein, E. L. Gurevich, E. P. George, A. Ostendorf, G. Laplanche, "Laser metal deposition of a refractory TiZrNbHfTa high-entropy alloy," *Additive Manufacturing*, vol. 24, pp. 386–390, 2018. https://doi.10.1016/j.addma.2018.10.008

[43] W. Wang, J. Ning, S. Y. Liang, "Prediction of lack-of-fusion porosity in laser powder-bed fusion considering boundary conditions and sensitivity to laser power absorption". https://doi.10.1007/s00170-020-06224-7/Published

[44] S.J. Wolff, H. Wang, B. Gould, N. Parab, Z. Wu, C. Zhao et al., "In situ X-ray imaging of pore formation mechanisms and dynamics in laser powder-blown directed energy deposition additive manufacturing," *International Journal Machining and Tools Manufacturing*, vol. 166, p. 103743, 2021. https://doi.org/10.1016/j.ijmachtools.2021.103743

[45] A. Castellano, M. Mazzarisi, S. L. Campanelli, A. Angelastro, A. Fraddosio, M. D. Piccioni, "Ultrasonic characterization of components manufactured by direct laser metal deposition," *Materials*, vol. 13, no. 11, 2020. https://doi.10.3390/ma13112658

[46] M. S. Palm, B. Diepold, S. Neumeier, H. W. Hoeppel, M. Goeken, M. F. Zaeh, "Detection and effects of lack of fusion defects in Hastelloy X manufactured by laser powder bed fusion," *Materials and Design,* vol. 230, 2023. https://doi.10.1016/j.matdes.2023.111941

[47] M. Ilanlou, R. Shoja Razavi, S. Haghighat, A. Nourollahi, "Multi-track laser metal deposition of Stellite6 on martensitic stainless steel: Geometry optimization and defects suppression," *Journal of Manufacturing Processes*, vol. 86, pp. 177–186, 2023. https://doi.10.1016/j.jmapro.2022.12.036

[48] H. Ouidadi, S. Guo, C. Zamiela, L. Bian, "Real-time defect detection using online learning for laser metal deposition," *Journal of Manufacturing Processes.*, vol. 99, pp. 898–910,2023. https://doi.10.1016/j.jmapro.2023.05.030

[49] S. Webster, N. Moser, K. Fezzaa, T. Sun, K. Ehmann, E. Garboczi et al., "Pore formation driven by particle impact in laser powder-blown directed energy deposition," *PNAS Nexus*, vol. 2, no. 6, p. pgad178, 2023. https://doi.org/10.1093/pnasnexus/pgad178

[50] H. Dobbelstein, E. P. George, E. L. Gurevich, A. Kostka, A. Ostendorf, G. Laplanche, "Laser metal deposition of refractory high-entropy alloys for high-throughput synthesis and structure-property characterization," *International Journal of Extreme Manufacturing*, vol. 3, no. 1, 2020. https://doi.10.1088/2631-7990/abcca8

[51] A. Salmi, G. Piscopo, A. N. Pilagatti, E. Atzeni, "Evaluation of Porosity in AISI 316L Samples Processed by Laser Powder Directed Energy Deposition," *Journal of Manufacturing and Materials Processing*, vol. 8, no. 4, 2024. https://doi.10.3390/jmmp8040129

[52] M. Yeganeh, Z. Shahryari, A. Talib Khanjar, Z. Hajizadeh, F. Shabani, "Inclusions and Segregations in the Selective Laser-Melted Alloys: A Review" *Multidisciplinary Digital Publishing Institute (MDPI)*. https://doi.10.3390/coatings13071295

[53] B. Borges, L. Quintino, R. M. Miranda, P. Carr, "Imperfections in laser cladding with powder and wire fillers," *International Journal of Advanced Manufacturing Technology*, vol. 50, no. 1–4, pp. 175–183, 2010, https://doi.10.1007/s00170-009-2480-2

[54] G. Dursun, S. Ibekwe, G. Li, P. Mensah, G. Joshi, D. Jerro, "Influence of laser processing parameters on the surface characteristics of 316L stainless steel manufactured by selective laser melting," in *Materials Today: Proceedings*, Elsevier Ltd, 2019, pp. 387–393. https://doi.10.1016/j.matpr.2019.12.061

[55] A. S. , D. W. R. D. , A. Jain, J. Kandasamy, M. Singhal, "Laser processing techniques for surface property enhancement: Focus on material advancement," 2023, *Elsevier B.V.* doi: 10.1016/j.surfin.2023.103293

[56] G. K. L. Ng, G. Bi, K. M. Teh, H. Zheng," An investigation on porosity in laser metal deposition," in *ICALEO 2008 - 27th International Congress on Applications of Lasers and Electro-Optics, Congress Proceedings*, Laser Institute of America, 2008, pp. 23–30. https://doi.10.2351/1.5061227

[57] G. P. Dinda, L. Song, J. Mazumder, “Fabrication of Ti-6Al-4V scaffolds by direct metal deposition,” *Metallurgical and Materials Transactions, A Phys. Metall. Mater. Sci.*, vol. 39, no. 12, pp. 2914–2922, 2008. https://doi.10.1007/s11661-008-9634-y

[58] A. V. Gusarov, M. Pavlov, I. Smurov, “Residual stresses at laser surface remelting and additive manufacturing,” in *Physics Procedia*, Elsevier B.V., 2011, pp. 248–254. https://doi.10.1016/j.phpro.2011.03.032

[59] M. Qu, Q. Guo, L. I. Escano, S. J. Clark, K. Fezzaa, L. Chen, “Mitigating keyhole pore formation by nanoparticles during laser powder bed fusion additive manufacturing,” *Additive Manufacturing Letters*, vol. 3, 2022. https://doi.10.1016/j.addlet.2022.100068

[60] S.M.H. Hojjatzadeh, N.D. Parab, Q. Guo, M. Qu, L. Xiong, C. Zhao, et al., “Direct observation of pore formation mechanisms during LPBF additive manufacturing process and high energy density laser welding,” *International Journal Machining and Tools Manufacturing*, vol. 153, p. 103555, 2020. https://doi.org/10.1016/j.ijmachtools.2020.103555

[61] H. Rezaeifar, M. Elbestawi, “Porosity formation mitigation in laser powder bed fusion process using a control approach,” *Optics and Laser Technology*, vol. 147,2022. https://doi.10.1016/j.optlastec.2021.107611.

[62] M. Ghasempour-Mouziraji, J. Lagarinhos, D. Afonso, R. Alves de Sousa, “A review study on metal powder materials and processing parameters in Laser Metal position,” 2024. *Elsevier Ltd*. https://doi.10.1016/j.optlastec.2023.110226

[63] K. Zhang, X. Zhang,W. Liu, “Effects of processing parameters on powder utilization ratio during laser metal deposition shaping,” in *Advanced Materials Research*, 2012, pp. 790–794. https://doi.10.4028/www.scientific.net/AMR.549.790

[64] J. Hofman, “Development of an observation and control system for industrial laser cladding,” PhD Thesis, Materials Innovation Institute M2i, Netherlands, 2009. https://doi.org/10.3990/1.9789077172421

[65] W. Li, H. Yang, Y. Liu, F. Li, J. Yi, J. Eckert, “Effect of laser power on microstructure and properties of WC-12Co composite coatings deposited by laser-based directed energy deposition,” *Materials*, vol. 17, no. 17, 2024. https://doi.10.3390/ma17174215

[66] Z. Qi, Y. Li, X. Chu, Y. Xie, Y. Long, “Effect of laser power on microstructure and properties of laser assisted cold sprayed copper coatings on steel,” *Surface and Coating Technology*, vol. 477, 2024. https://doi.10.1016/j.surfcoat.2023.130308

[67] Z. Wang, J. Zhang, F. Zhang, C. Qi, “Impact of laser energy density on the structure and properties of laser-deposited Fe–Ni–Ti composite coatings,” *Frontiers in Materials*, vol. 11, 2024. https://doi.10.3389/fmats.2024.1408333

[68] X. Liu, L. Meng, X. Zeng, B. Zhu, K. Wei, J. Cao, et al., “Studies on high power laser cladding Stellite 6 alloy coatings: Metallurgical quality and mechanical performances,” Surface Coating Technology, vol. 481, p. 130647, 2024. https://doi.org/10.1016/j.surfcoat.2024.130647

[69] Z. Uddin, M. M. Butt, V. Kvvssn, M. U. Salamci, H. Kizil, “Understanding the effects of manufacturing attributes on damage tolerance of additively manufactured parts and exploring synergy among process-structure-properties. A comprehensive review,” *John Wiley and Sons Inc*., 2024. https://doi.10.1002/eng2.13020

[70] X. Chen, C. Zhao, X. Zhu, G. Yin, Y. Xu, “Effect of scanning speeds on microstructure evolution and properties of 70Cr8Ni2Y coatings by direct laser deposition,” *Material Research Express*, vol. 11, no. 9, 2024. https://doi.10.1088/2053-1591/ad78af

[71] Y. Jian, Y. Liu, H. Qi, P. He, G. Huang, Z. Huang, “Effects of scanning speed on the microstructure, hardness and corrosion properties of high-speed laser cladding Fe-based stainless coatings,” *Journal of Materials Research and Technology*, vol. 29, pp. 3380–3392,2024. https://doi.10.1016/j.jmrt.2024.02.087

[72] C. Hicks, T. Konkova, P. Blackwell, “Influence of laser power and powder feed rate on the microstructure evolution of laser metal deposited Ti-5553 on forged substrates,” *Materials Characterization, vol. 170, 2020*. https://doi.10.1016/j.matchar.2020.110675

[73] T. G. Kim, D. S. Shim, “Effect of laser power and powder feed rate on interfacial crack and mechanical/microstructural characterizations in repairing of 630 stainless steel using direct energy deposition,” *Materials Science and Engineering: A*, vol. 828, 2021. https://doi.10.1016/j.msea.2021.142004

[74] A. K. Maurya, A. Kumar, S. K. Saini, C. P. Paul, “Study of build rate in laser directed energy deposition,” *Manufacturing Technology Today (MTT)*, vol. 22, no. 1, pp. 39–44, 2023. https://doi.10.58368/mtt.22.1.2023.39-44

[75] Y. Kong, L. Zhao, L. Zhu, H. Huang, “The selection of laser beam diameter in directed energy deposition of austenitic stainless steel: A comprehensive assessment,” *Additive Manufacturing*, vol. 52, 2022. https://doi.10.1016/j.addma.2022.102646

[76] A. Vidergar, A. Jeromen, E. Govekar, “Influence of the laser-beam intensity distribution on the performance of directed energy deposition of an axially fed metal powder,” *Journal of Materials Processes and Technology*, vol. 327, 2024. https://doi.10.1016/j.jmatprotec.2024.118360

[77] C. Hong, B. Burbaum, A. Gasser, I. Kelbassa, “Advantages of laser metal deposition by using zoom optics and MWO (Modular Welding Optics),” in *30th International Congress on Applications of Lasers and Electro-Optics, ICALEO 2011*, Laser Institute of America, 2011, pp. 295–300. https://doi.10.2351/1.5062249

[78] S. Brudler, A.E. Medvedev, C. Pandelidi, S. Piegert, T. Illston, M. Qian et al., “Systematic investigation of performance and productivity in laser powder bed fusion of Ti6Al4V up to 300 µm layer thickness,” *Journal Material Process Technology*, vol. 330, p. 118450, 2024. https://doi.org/10.1016/j.jmatprotec.2024.118450

[79] S. Li, G. Fu, H. Li, Z. Ren, S. Li, H. Xiao et al., “Effect of layer thickness on the melt pool behavior and pore defects evolution of selective laser melting CuCrZr alloy,” *Journal Alloys and Compound*, vol. 967, p. 171778, 2023. https://doi.org/10.1016/j.jallcom.2023.171778

[80] N. Rońda, K. Grzelak, M. Polański, J. Dworecka-Wójcik, “The Influence of Layer Thickness on the Microstructure and Mechanical Properties of M300 Maraging Steel Additively Manufactured by LENS® Technology,” *Materials*, vol. 15, no. 2, 2022, https://doi.10.3390/ma15020603

[81] X. Bu, X. Xu, H. Lu, Y. Liang, H. Bian, K. Luo et al.,” Effect of overlap rate on the microstructure and properties of Cr-rich stainless-steel coatings prepared by extreme high-speed laser cladding,” *Surface Coating Technology*, vol. 487, p. 131025, 2024. https://doi.org/10.1016/j.surfcoat.2024.131025

[82] C. Ding, Q. Zhang, S. Sun, H. Ni, Y. Liu, X. Wang et al., “Effect of laser energy density on the properties of CoCrFeMnNi high-entropy alloy coatings on steel by laser cladding,” *Metals* (Basel), vol. 14, no. 9, p. 997, 2024. https://doi.org/10.3390/met14090997

[83] G. Shao, J. Lei, F. Zhang, S. Wang, H. Hu, K. Wang et al., “A study of the microstructure and mechanical and electrochemical properties of CoCrFeNi high-entropy alloys additive-manufactured using laser metal deposition,” *Coatings*, vol. 13, no. 9, p. 1583, 2023. https://doi.org/10.3390/coatings13091583.

[84] B. Preuß, T. Lindner, T. Uhlig, T. Mehner, G. Töberling, G. Wagner et al., “Wear and corrosion resistant eutectic high-entropy alloy Al0.3CoCrFeNiMo0.75 produced by laser metal deposition and spark-plasma sintering,” *Journal of Thermal Spray Technology*, vol. 33, no. 2–3, pp. 489–503, 2024. https://doi.org/10.1007/s11666-024-01711-9

[85] O. Prakash, R. Chandrakar, L. Martin, J. Verma, A. Kumar, A. Jaiswal, “Laser cladding technology for high entropy alloys: effect and applications,” *Material Research Express*, vol. 11, no. 9, 2024. https://doi.10.1088/2053-1591/ad75e8

[86] N. Gong, T.L. Meng, J. Cao, Y. Wang, R. Karyappa, C.K. Ivan Tan et al., “Laser-cladding of high entropy alloy coatings: an overview,” *Materials Technology*, vol. 38, no. 1, p. 2151696, 2023. https://doi.org/10.1080/10667857.2022.2151696

[87] J. P. Oliveira, A. D. LaLonde, J. Ma, “Processing parameters in laser powder bed fusion metal additive manufacturing,” *Materials and Design*, vol. 193, Aug. 2020. https://doi.10.1016/j.matdes.2020.108762

[88] J. I. Arrizubieta, A. Lamikiz, F. Klocke, S. Martínez, K. Arntz, E. Ukar, “Evaluation of the relevance of melt pool dynamics in Laser Material Deposition process modeling’, *Interntaional Journal of Heat Mass Transfer*, vol. 115, pp. 80–91, 2017.https://doi.10.1016/j.ijheatmasstransfer.2017.07.011

[89] M. Dada, P. Popoola, N. Mathe, S. Pityana, S. Adeosun, “Effect of laser parameters on the properties of high entropy alloys: A preliminary study,” in *Materials Today: Proceedings*, Elsevier Ltd, 2021. pp. 756–761. https://doi.10.1016/j.matpr.2020.04.198

[90] D. Svetlizky, M. Das, B. Zheng, A.L. Vyatskikh, S. Bose, A. Bandyopadhyay, et al., “Directed energy deposition (DED) additive manufacturing: Physical characteristics, defects, challenges and applications,” Materials Today, Elsevier B.V., vol. 49, p. 271–295, 2021. https://doi.org/10.1016/j.mattod.2021.03.020

[91] R. Sampson, R. Lancaster, M. Sutcliffe, D. Carswell, C. Hauser, J. Barras, “The influence of key process parameters on melt pool geometry in direct energy deposition additive manufacturing systems,” *Optic and Laser Technology*, vol. 134, 2021. https://doi.10.1016/j.optlastec.2020.106609

[92] J. C. Haley, J. M. Schoenung, E. J. Lavernia, “Observations of particle-melt pool impact events in directed energy deposition,” *Additive Manufacturing*, vol. 22, pp. 368–374, 2018. https://doi.10.1016/j.addma.2018.04.028

[93] A. R. Riensche, B. D. Bevans, G. King, A. Krishnan, K. D. Cole, P. Rao, “Predicting meltpool depth and primary dendritic arm spacing in laser powder bed fusion additive manufacturing using physics-based machine learning,” *Materials Design*, vol. 237, p. 112540, 2024. https://doi.org/10.1016/j.matdes.2023.112540

[94] A. Azizi, F. Hejripour, J.A. Goodman, P.A. Kulkarni, X. Chen, G. Zhou et al., “Process-dependent anisotropic thermal conductivity of laser powder bed fusion AlSi10Mg: impact of microstructure and aluminum-silicon interfaces,” Rapid Prototyp Journal. vol. 29, no. 6, pp. 1109–1120, 2023. https://doi.org/10.1108/RPJ-09-2022-0290

[95] T. Liu, Z. Gao, W. Ling, Y. Wang, X. Wang, X. Zhan, “Effect of heat accumulation on the microstructure of Invar alloy manufactured by multi-layer multi-pass laser melting deposition,” *Optic and Laser Technology*, vol. 144, 2021. https://doi: 10.1016/j.optlastec.2021.107407

[96] C. Hagenlocher, P. O’Toole, W. Xu, M. Brandt, M. Easton, A. Molotnikov, “The effect of heat accumulation on the local grain structure in laser-directed energy deposition of aluminium,” *Metals (Basel).*, vol. 12, no. 10, 2022. https://doi: 10.3390/met12101601

[97] R. M. Mahamood, E. T. Akinlabi, M. Shukla, S. Pityana, “Scanning velocity influence on microstructure, microhardness and wear resistance performance of laser deposited Ti6Al4V/TiC composite,” *Material Designs*, vol. 50, pp. 656–666, 2013. https://doi.10.1016/j.matdes.2013.03.049

[98] Y. Lee, E.S. Kim, S. Park, J.M. Park, J.B. Seol, H.S. Kim et al., “Effects of laser power on the microstructure evolution and mechanical properties of Ti–6Al–4V alloy manufactured by direct energy deposition,” *Metals and Materials International*, vol. 28, no. 1, pp. 197–204, 2022. https://doi.org/10.1007/s12540-021-01081-9

[99] M. Dada, P. Popoola, N. Mathe, S. Pityana, S. Adeosun, "In-situ reactive synthesis and characterization of a high entropy alloy coating by laser metal deposition," *International Journal of Lightweight Materials and Manufacture*, vol. 5, no. 1, pp. 11–19, 2022. https://doi.10.1016/j.ijlmm.2021.09.002
[100] C. Bernauer, L. Meinzinger, A. Zapata, X. F. Zhao, S. Baehr, M. F. Zaeh, "Design and investigation of a novel local shielding gas concept for laser metal deposition with coaxial wire feeding," *Applied Sciences (Switzerland)*, vol. 13, no. 8, 2023. https://doi.10.3390/app13085121
[101] M. Dada, P. Popoola, N. Mathe, S. Pityana, S. Adeosun, "Parametric optimization of laser deposited high entropy alloys using response surface methodology (RSM)," *International Journal of Advanced Manufacturing Technology*, vol. 109, no. 9–12, pp. 2719–2732, 2020. https://doi.10.1007/s00170-020-05781-1
[102] M. Bensouici, M. W. Azizi, F. Z. Bensouici, "Performance Analysis and Optimization of Regenerative Gas Turbine Power Plant using RSM," *International Journal of Automotive and Mechanical Engineering*, vol. 20, no. 3, pp. 10671–10683, 2023. https://doi.10.15282/ijame.20.3.2023.10.0824
[103] M. N. Nezhad, M. R. Aboutalebi, S. H. Seyedein, M. Barekat, "Multi-criteria optimization of processing parameters in laser cladding of Al0.5CoCrFeNiNb0.5-Si0.1 high entropy alloy coating," *Journal of Materials Research and Technology*, vol. 35, pp. 6519–6536, 2025. https://doi.10.1016/j.jmrt.2025.02.239
[104] L. Que, G. Lian, M. Yao, H. Lu, "Microstructure and properties of AlCoCrFeNiTi high-entropy alloy coatings prepared by laser cladding based on the response surface methodology," *International Journal of Advanced Manufacturing Technology*, vol. 123, no. 3–4, pp. 1307–1321, 2022. https://doi.10.1007/s00170-022-10225-z
[105] A. A. Akinwande, O. A. Balogun, A. A. Adediran, O. S. Adesina, V. Romanovski, T. C. Jen, "Experimental analysis, statistical modelling, and parametric optimization of quinary-(CoCrFeMnNi)100 –x/TiCx high-entropy-alloy (HEA) manufactured by laser additive manufacturing," *Results in Engineering*, vol. 17, 2023. https://doi. 10.1016/j.rineng.2022.100802
[106] B. Jiang, Z. Huang, C. Liu, H. Wang, F. Shu, Y. Zhao et al., "Optimization of process parameters and microstructure of CoCrFeNiTiAl high-performance high-entropy alloy coating," Metals (Basel), vol. 14, no. 12, p. 1384, 2024. https://doi.org/10.3390/met14121384
[107] Y. Huang, Y. Hu, M. Zhang, C. Mao, K. Wang, Y. Tong et al., "Multi-objective optimization of process parameters in laser cladding CoCrCuFeNi high-entropy alloy coating," Journal of Thermal Spray Technology, vol. 31, p. 1985–2000, 2022. https://doi.org/10.1007/s11666-022-01408-x
[108] Z. Dong, L. Feng, H. Long, B. Lu, J. Zhu, and X. Yan et al., "A multi-objective optimization of laser cladding processing parameters of AlCoCrFeNi2.1 eutectic high-entropy alloy coating," Optic and Laser Technology, vol. 170, p. 110302, 2024. https://doi.org/10.1016/j.optlastec.2023.110302
[109]] B. Xiao, J. Li, S. Li, A. Wang, H. Fu, H. Zhang et al., "Process optimization and microstructure of Ti3Zr1.5NbVAl0.25 high entropy alloy produced by directed energy deposition," Materials Characteristic, vol. 215, p. 114147, 2024. https://doi.org/10.1016/j.matchar.2024.114147
[110] B. Duan, H. Zhao, N. Lin, L. Zhou, X. Wang, G. Ma et al., "Predictive modelling and process optimisation of high-speed laser cladding FeCrNiMo0.75 alloy coating on 45# steel," Materials Today Communication, vol. 44, p. 112107, 2025. https://doi.org/10.1016/j.mtcomm.2025.112107
[111] S. Gao, Q. Fu, M. Li, L. Huang, N. Liu, C. Cui et al., "Optimization of laser cladding parameters for high-entropy alloy-reinforced 316L stainless-steel via grey relational analysis," Coatings, vol. 14, no. 9, p. 103, 2024. https://doi.org/10.3390/coatings14091103
[112] T. Zulkifli, Z. Djafar, M. Massaguni, "Multi-factorial analysis and optimization of delamination damage parameters in the drilling of woven ramie/epoxy resin composite," *International Journal of Automotive and Mechanical Engineering*, vol. 23, no. 1, pp. 13356–13366, 2026 https://doi.10.15282/ijame.23.1.2026.15.1013
[113] Y. Liu, C. Liu, W. Liu, Y. Ma, S. Tang, C. Liang et al., "Optimization of parameters in laser powder deposition AlSi10Mg alloy using Taguchi method," Optic and Laser Technology, vol. 111, pp. 470–480, 2019. https://doi.org/10.1016/j.optlastec.2018.10.030
[114] J. Y. Zhong, J. J. Wang, F. Y. Ouyang, "Optimization of Sputtering Process for Medium Entropy Alloy Nanotwinned CoCrFeNi Thin Films by Taguchi Method," *Materials*, vol. 15, no. 22, 2022. https://doi.10.3390/ma15228238
[115] L. J. J. Kumar, G. G. K. Nair, "Laser Metal Deposition Repair Applications for Ti-6Al-4V Alloy," *Mechanics, Materials Science & Engineering Journal*, vol. 7, 2017, https://doi.10.13140/RG.2.2.35949.38889
[116] A. Huang, Y. Liu, X. Li, J. Liu, S. Yang, "Numerical Simulation of Temperature Field, Velocity Field and Solidification Microstructure Evolution of Laser Cladding AlCoCrFeNi High Entropy Alloy Coatings," *Lubricants*, vol. 13, no. 12, 2025, https://doi.10.3390/lubricants13120541
[117] L.R. Kanyane, P. Lepele, N. Malatji, M.B. Shongwe, "3D finite element analysis and experimental correlations of laser synthesized AlCrNiTiNb high entropy alloy coating," *Materials Today Communication*, vol. 38, p. 107686, 2024. https://doi.org/10.1016/j.mtcomm.2023.107686
[118] C. Chen, X. Cong, J. Liu, H. Zhang, "Influences of Heat Input on the Geometric Parameters and Element Distribution of CrMnFeCoNi High-Entropy Alloy Coating on Aluminum Alloy Using Laser Cladding," *Transactions of the Indian Institute of Metals*, vol. 76, no. 5, pp. 1271–1280, 2023. https://doi.10.1007/s12666-022-02825-w
[119] J. Gao, X. Wang, C. Wang, Y. Hao, X. Liang, W. Li et al., "Multi-objective optimization of process parameters for laser metal deposition of NiTi shape memory alloy based on neural network and genetic algorithm,"

International Journal of Advanced Manufacturing Technology, vol. 130, no. 9–10, pp. 4663–4678, 2024. https://doi.org/10.1007/s00170-024-12974-5

[120] P. Xue, L. Zhu, P. Xu, Y. Ren, B. Xin, and G. Meng et al. "Research on process optimization and microstructure of CrCoNi medium-entropy alloy formed by laser metal deposition," *Optic and Laser Technology*, vol. 142, p. 107167, 2021. https://doi.org/10.1016/j.optlastec.2021.107167

[121] H. Hassanin, M.A. El-Sayed, M. Ahmadein, N.A. Alsaleh, S. Ataya, M.M.Z. Ahmed et al., "Optimising surface roughness and density in titanium fabrication via laser powder bed fusion," Micromachines (Basel), vol. 14, no. 8, 2023. https://doi.org/10.3390/mi14081642

[122] Q. Gao, H. Liu, P. Chen, X. Liu, H. Yang, J. Hao, 'Multi-objective optimization for laser cladding refractory MoNbTiZr high-entropy alloy coating on Ti6Al4V', *Optic and Laser Technology*, vol. 161,2023. https://doi.10.1016/j.optlastec.2023.109220

[123] A.A. Siddiqui, A.K. Dubey, C.P. Paul, "Geometrical characteristics in laser surface alloying of a high-entropy alloy," *International Journal of Lasers in Engineering*, vol. 14, pp. 237-259, 2018

[124] M. Ansari, R. Shoja Razavi, M. Barekat, "An empirical-statistical model for coaxial laser cladding of NiCrAlY powder on Inconel 738 superalloy," *Optic and Laser Technology*, vol. 86, pp. 136–144, 2016 https://doi.10.1016/j.optlastec.2016.06.014

[125] J. K. Jatavallabhula, V. R. Veeredhi, G. S. Reddy, R. R. Baridula, V. V. Satyanarayana, "Machine Learning-Based Prediction of Impact Toughness in AISI 430–AISI 304 Friction-Welded Joints," *International Journal of Automotive and Mechanical Engineering*, vol. 22, no. 1, pp. 12118–12132, 2025. https://doi.10.15282/ijame.22.1.2025.13.0930

[126] T. Wang, Y. Li, T. Li, B. Liu, X. Li, X. Zhang, "Machine learning in additive manufacturing: enhancing design, manufacturing and performance prediction intelligence," *Journal Intelligent Manufacturing*, 2025. https://doi.10.1007/s10845-025-02568-7

[127] D. O. Kim, C. M. Lee, D. H. Kim, "Determining optimal bead central angle by applying machine learning to wire arc additive manufacturing (WAAM)," *Heliyon*, vol. 10, no. 1, 2024, https://doi.10.1016/j.heliyon.2023.e23372.

[128] J. A. Lee, M. J. Sagong, J. Jung, E. S. Kim, H. S. Kim, "Explainable machine learning for understanding and predicting geometry and defect types in Fe-Ni alloys fabricated by laser metal deposition additive manufacturing," *Journal of Materials Research and Technology*, vol. 22, pp. 413–423, 2023. https://doi.10.1016/j.jmrt.2022.11.137

[129] D. Zhang, Z. Liu, K. Song, Z. Zhai, Y. Zhang, Z. Gao, "Parameters optimization for laser-cladding CoCrFeNiMn high-entropy alloy layer based on GRNN and NSGA-II," *Material Today Communication*, vol. 39, 2024. https://doi.10.1016/j.mtcomm.2024.108615

[130] H. Cheng, H. Luo, C. Fan, X. Wang, C. Li, "Accelerated design of high-entropy alloy coatings for high corrosion resistance via machine learning," *Surface Coating Technology*, vol. 502, 2025, https://doi.10.1016/j.surfcoat.2025.131978

[131] S. Lin, Y. Yao, G. Shi, Y. Liu, Z. Yao, S. Lu et al., "Machine learning-driven design of BCC phase FeCrVTiMoxSiy high-entropy alloy coatings with high hardness to enhance wear resistance," *Surface Coating Technology*, vol. 511, 2025. https://doi.org/10.1016/j.surfcoat.2025.132238

[132] V. Diwakar, A. Sharma, M. Z. K. Yusufzai, M. Vashista, "Machine learning-based prediction of single clad characteristics and non-destructive characterization of multi-layer deposited FeCoNiCrMo HEA on EN24 via laser cladding," *Material Today Communication*, vol. 41, 2024. https://doi.10.1016/j.mtcomm.2024.110839

[133] S. Hosseini, E. Vaghefi, C. Lee, B. Prorok, E. Mirkoohi, "Machine learning-enabled prediction and optimization of hardness for Nb-Ti-V-Zr refractory high entropy alloy" *Material Today Communication*, vol. 40, 2024. https://doi.10.1016/j.mtcomm.2024.109607

[134] M. Asad, U. Iftikhar, D. Abbasi, M. B. Jamil, "A comparative analysis of regression modelling and artificial neural networks for diesel engine performance prediction," *International Journal of Automotive and Mechanical Engineering*, vol. 23, no. 1, pp. 13339–13355, 2026. htpps://doi.10.15282/ijame.23.1.2026.13.1011

[135] S. Sivaraman, N. Radhika, M.A. Khan, "Machine learning-driven prediction of wear rate and phase formation in high entropy alloy coatings for enhanced durability and performance," *IEEE Access*, vol. 13, pp. 33956–33975, 2025. https://doi.org/10.1109/access.2025.3542507

[136] H. Liu, F. Ding, P. Chen, J. Hao, R. Geng, X. Liu, "Phase prediction in laser-clad high-entropy alloy coatings through metaheuristic optimization algorithms and interpretable machine learning," *Materials Chemistry and Physics*, vol. 332, p. 130282, 2025. https://doi.org/10.1016/j.matchemphys.2024.130282

[137] S.G. Ghalme, I. Momohjimoh, Y. Falak, R.K. Thakur, "Investigation of mechanical properties of groundnut-based composite using the entropy-weighted TOPSIS approach," *International Journal of Automotive and Mechanical Engineering*, vol. 22, no. 1, pp. 12062–12073, 2025. https://doi.org/10.15282/ijame.22.1.2025.9.0926

[138] X. Shang, A. Talbot, E. Li, H. Wen, T. Lyu, J. Zhang et al., "Accurate inverse process optimization framework in laser directed energy deposition," *Additive Manufacturing*, vol. 102, p. 104736, 2025. https://doi.org/10.1016/j.addma.2025.104736

[139] M. Perani, R. Jandl, S. Baraldo, A. Valente, B. Paoli, "Long-short term memory networks for modelling track geometry in laser metal deposition," *Front Artificial Intelligence*, vol. 6, 2023. https://doi.org/10.3389/frai.2023.1156630

[140] A. Hamrani, A. Medarametla, D. John, A. Agarwal, “Machine-learning-driven optimization of cold spray process parameters: Robust inverse analysis for higher deposition efficiency,” *Coatings*, vol. 15, no. 1, p. 12, 2025. https://doi.org/10.3390/coatings15010012

[141] P.A. Adedeji, S.A. Akinlabi, N. Madushele, O.O. Olatunji, “Hybrid neurofuzzy wind power forecast and wind turbine location for embedded generation,” *International Journal of Energy Research*, vol. 45, no. 1, pp. 413–28, 2021. https://doi.org/10.1002/er.5620

[142] J. Li, D. Du, X. Yang, Y. Qiu, S. Xiang, “Determining Homogenization Parameters and Predicting 5182-Sc-Zr Alloy Properties by Artificial Neural Networks,” *Materials*, vol. 16, no. 15, 2023. doi: 10.3390/ma16155315

[143] V. Wong, A. Aversa, A. R. Rodrigues, “A deep learning model for estimating the quality of bimetallic tracks obtained by laser powder-directed energy deposition,” *Materials*, vol. 17, no. 22, 2024. https://doi.10.3390/ma17225653